EUROPEAN RESPIRATORY *journal*

FLAGSHIP SCIENTIFIC JOURNAL OF ERS

Early View

Original article

Cigarette smoke-initiated autoimmunity facilitates sensitisation to elastin-induced COPD-like pathologies in mice

Jie-Sen Zhou, Zhou-Yang Li, Xu-Chen Xu, Yun Zhao, Yong Wang, Hai-Pin Chen, Min Zhang, Yin-Fang Wu, Tian-Wen Lai, Chun-Hong Di, Ling-Ling Dong, Juan Liu, Nan-Xia Xuan, Chen Zhu, Yan-Ping Wu, Hua-Qiong Huang, Fu-Gui Yan, Wen Hua, Yi Wang, Wei-Ning Xiong, Hui Qiu, Tao Chen, Dong Weng, Hui-Ping Li, Xiaobo Zhou, Lie Wang, Fang Liu, Xin Lin, Song-Min Ying, Wen Li, Mitsuru Imamura, Mary E. Choi, Martin R. Stampfli, Augustine M.K. Choi, Zhi-Hua Chen, Hua-Hao Shen

Please cite this article as: Zhou J-S, Li Z-Y, Xu X-C, *et al*. Cigarette smoke-initiated autoimmunity facilitates sensitisation to elastin-induced COPD-like pathologies in mice. *Eur Respir J* 2020; in press (https://doi.org/10.1183/13993003.00404-2020).

Cigarette smoke-initiated autoimmunity facilitates sensitization to elastin-induced COPD-like pathologies in mice

Jie-Sen Zhou[1, #], Zhou-Yang Li[1, #], Xu-Chen Xu[1], Yun Zhao[1], Yong Wang[1], Hai-Pin Chen[1], Min Zhang[1], Yin-Fang Wu[1], Tian-Wen Lai[1], Chun-Hong Di[2], Ling-Ling Dong[1], Juan Liu[1], Nan-Xia Xuan[1], Chen Zhu[1], Yan-Ping Wu[1], Hua-Qiong Huang[1], Fu-Gui Yan[1], Wen Hua[1], Yi Wang[3], Wei-Ning Xiong[3], Hui Qiu[4], Tao Chen[4], Dong Weng[4], Hui-Ping Li[4], Xiaobo Zhou[5], Lie Wang[6], Fang Liu[7], Xin Lin[7], Song-Min Ying[1], Wen Li[1], Mitsuru Imamura[8], Mary E. Choi[9], Martin R. Stampfli[10,11], Augustine M.K. Choi[8, *], Zhi-Hua Chen[1, *], Hua-Hao Shen[1, 11, *]

[1]Key Lab of Respiratory Disease of Zhejiang Province, Department of Respiratory and Critical Care Medicine, Second Affiliated Hospital, Zhejiang University School of Medicine, Hangzhou, China.

[2]Department of Clinical Laboratory, the Affiliated Hospital of Hangzhou Normal University, Hangzhou, China.

[3]Department of Respiratory and Critical Care Medicine, Key Laboratory of Pulmonary Diseases of Health Ministry, Tongji Hospital, Tongji Medical College, Huazhong University of Sciences & Technology, Wuhan, China.

[4]Department of Respiratory Medicine, Shanghai Pulmonary Hospital, Tongji University School of Medicine, Shanghai, China.

[5]Channing Laboratory, Brigham and Women's Hospital, Harvard Medical School, Boston, USA.

[6]Institute of Immunology, Zhejiang University School of Medicine, Hangzhou, China.

[7]Institute for Immunology, Tsinghua University School of Medicine, Tsinghua University-Peking University Jointed Center for Life Sciences, Beijing, China.

[8]Division of Pulmonary and Critical Care Medicine, and [9]Division of Nephrology and Hypertension, Joan and Sanford I. Weill Department of Medicine, New York–Presbyterian Hospital, Weill Cornell Medical College, New York, USA.

[10]Department of Pathology and Molecular Medicine, McMaster Immunology Research Centre, and Department of Medicine, Firestone Institute for Respiratory Health at St. Joseph's Healthcare,

McMaster University, Hamilton, Ontario, Canada.

[11]State Key Lab of Respiratory Disease, National Clinical Research Center for Respiratory Disease, Guangzhou, China.

[#]These authors contribute equally to this work

[*]Correspondence should be addressed to H.H.S. (huahaoshen@zju.edu.cn), Z.H.C. (zhihuachen@zju.edu.cn), or A.M.K.C. (amc2056@med.cornell.edu).

Correspondence

Hua-Hao Shen, MD. PhD, Department of Respiratory and Critical Care Medicine, Key Laboratory of Respiratory Disease of Zhejiang Province, Second Affiliated Hospital, Zhejiang University School of Medicine, 88 Jiefang Rd., Hangzhou 310009, China. Tel.: 86-571-8898-1913; Fax: 86-571-8778-3729

Take home message

MMP12-generated elastin fragments serve as a self-antigen and drive CS-induced autoimmune processes in mice. These findings provide experimental evidence for cigarette smoke-induced autoimmunity and represent a novel mouse model of COPD.

ABSTRACT

It is currently not understood whether cigarette smoke (CS) exposure facilitates sensitization to self-antigens and whether ensuing auto-reactive T cells drive COPD-associated pathologies.

To address this question, mice were exposed to CS for 2 weeks. Following a two-week period of rest, mice were challenged intratracheally with elastin for 3 days or 1 month. *Rag1*$^{-/-}$, *Mmp12*$^{-/-}$, and *Il17a*$^{-/-}$ mice and neutralizing antibodies against active elastin fragments were used for mechanistic investigations. Human GVAPGVGVAPGV/HLA-A*02:01 tetramer was synthesized to assess the presence of elastin-specific T cells in patients with COPD.

We observed that 2 weeks of CS exposure induced an elastin-specific T cell response that led to neutrophilic airway inflammation and mucus hyperproduction following elastin recall challenge. Repeated elastin challenge for 1 month resulted in airway remodeling, lung function decline, and airspace enlargement. Elastin-specific T cell recall responses were dose dependent and memory lasted for over 6 months. Adoptive T cell transfer and studies in T cells deficient *Rag1*$^{-/-}$ mice conclusively implicated T cells in these processes. Mechanistically, CS exposure induced elastin-specific T cell responses were MMP12-dependent, while the ensuing immune inflammatory processes were IL17A-driven. Anti-elastin antibodies and T cells specific for elastin peptides were increased in patients with COPD.

These data demonstrate that MMP12-generated elastin fragments serve as a self-antigen and drive the CS-induced autoimmune processes in mice that result in a bronchitis-like phenotype and airspace enlargement. The study provides proof of concept of CS-induced autoimmune processes and may serve as a novel mouse model of COPD.

Introduction

COPD is a global public health concern. The disease encompasses two major clinical phenotypes, chronic bronchitis and emphysema. Cigarette smoking is the major risk factor of COPD, causing chronic airway inflammation, mucus hyperproduction, destruction of lung tissue, and remodelling of small airways. These processes contribute to largely irreversible airflow obstruction as well as systemic comorbidities [1, 2]. The cellular and molecular mechanisms that contribute to cigarette smoke (CS)-induced COPD pathogenesis remain largely unknown. Similarly, it is not well understood why airway inflammation persists in patients with COPD following smoking cessation [3].

It is widely accepted that CS exposure injures epithelial cells and activates alveolar macrophages, resulting in innate-driven inflammation. Moreover, CS exposure activates dendritic cells to induce adaptive immune response, including $CD4^+$ T cells, cytolytic $CD8^+$ T cells, and B cells. Together, these immune inflammatory processes to emphysema formation [4, 5]. It has been shown that the anti-elastin antibodies were present in patients with COPD [6, 7], and elastin peptides could act as cognate antigens to stimulate Th1- and Th17-polarized immune responses in subjects with emphysema [8]. These findings provide evidence that autoimmune processes may be implicated in the pathogenesis of COPD [9]. However, whether COPD indeed incorporates autoimmune disease processes remains controversial, as several groups did not observe increased anti-elastin antibodies in COPD [10, 11]. Moreover, CS-induced autoimmune processes have not been shown in experimental COPD models.

The objective of the current study was to investigate whether elastin serves as a self-antigen to drive CS-induced autoimmune processes. We show that CS-exposure facilitated sensitization to elastin through an MMP-12-dependent mechanism. Elastin challenge propagated T cell-dependent neutrophilic airway inflammation and induces COPD-like pathologies. Based on these findings, we propose that we established a rapid and novel autoimmune-driven mouse model that mimics most of the pathological features of human COPD.

Materials and methods

Additional details on methods are provided in an online data supplement.

Animals

6-8 weeks male C57BL/6 mice were purchased from the Animal Centre of Slaccas (Shanghai, China), *Rag1*$^{-/-}$ mice were purchased from Shanghai Model Organism (Shanghai, China), *Il17a*$^{-/-}$ mice were provided by the centre for Experimental Medicine and Systems Biology (Institute of Medical Science, University of Tokyo, Japan). *Mmp12*$^{-/-}$ mice were obtained from Jackson Laboratory (Maine, United States). All mice were maintained in the animal facility of the laboratory animal centre of Zhejiang University. Male mice aged 6-8 weeks were used for each experiment. All experimental protocols were approved by the Ethical Committee for Animal Studies at Zhejiang University.

In vivo CS exposures and treatments

Mice were exposed to CS in a stainless-steel chamber using a whole-body smoke exposure system (TE-10, Teague Enterprises) for approximately 2.5 h per day (100 cigarettes), 5 days per week. Total particulate matter concentrations in the exposure chamber were between 150-180 mg/m^3. Serum cotinine levels measured immediately after CS exposure were around 20 ng/ml. Control groups were exposed to filtered room air.

Mouse elastin (E6402-SPEC) was purchased from Sigma-Aldrich. 2 mg/ml elastin was suspended in sterile saline and sonicated. 100 μg elastin in 50 μl saline was administered intratracheally. For elastin sensitization, 100 μg elastin in 0.1 ml saline was mixed with 0.1ml complete Freund's adjuvant (CFA, F5881, Sigma-Aldrich) and injected intraperitoneally. BA4, a mouse monoclonal anti-elastin antibody (Sigma-Aldrich, E4013), 10 μg in 50 μl saline was instilled daily, 1 h before CS exposure.

Lipopolysaccharide (LPS: L2630, Sigma-Aldrich, 1 μg in 50 μl saline) was delivered intratracheally using a micro-syringe.

Human study subjects

We enrolled healthy controls and hospitalized COPD patients for collecting peripheral blood and

induced sputum. The diagnosis of COPD was made according to the GOLD (Global Initiative for Chronic Obstructive Lung Disease) guidelines [12]. Exclusion criteria were as follows: any chronic cardiopulmonary disease other than COPD and an inability to give written informed consent or cooperate with the study investigators. Clinical characteristics are described in Table 1. The study subjects were recruited from two medical centers. The study protocols were approved by the Ethics of Research Committee of the Second Affiliated Hospital, Zhejiang University. Written informed consent was obtained from all participants.

Table 1. Clinical characteristics of healthy controls and hospitalized COPD patients

Parameter	Healthy controls (n=20)	Smokers With COPD (n=17)	*P*
Age, y	59.15 ± 1.39	60.53 ± 1.47	0.501
Male, (%)	16 (80)	14 (82)	0.8604
Smoking, pack-years	NA	32.82±7.79	NA
BMI, kg/m^2	24.5±0.6	22.98±0.7	0.121
FEV$_1$, L	2.67±0.14	1.47±0.15	<0.001
FEV$_1$, % predicted	96.20±3.75	53.34±4.63	<0.001
FEV$_1$/FVC, %	83.60±2.02	52.05±2.65	<0.001
GOLD stage,			
I-II/III-IV, No. (%)	NA	8/9, (47/53)	NA
Sputum cell counts			
Eosinophils, %	0.12±0.05	0.38±0.18	0.040
Neutrophils, %	27.65±2.42	41.94±1.97	<0.001
Macrophages, %	72.03±2.40	57.65±2.28	<0.001
Lymphocytes, %	0.20±0.08	0.68±0.25	0.059
Treatment regimens, No. (%)			
ICS/LABA	NA	15, (88)	NA
LAMA	NA	4, (24)	NA
SABA	NA	10, (59)	NA
Theophylline	NA	12, (71)	NA

Data are presented as mean ± SEM. BMI: body mass index; FEV1: forced expiratory volume in the first second; FVC: forced vital capacity; ICS: inhaled corticosteroid; GOLD: global initiative for chronic obstructive lung disease; LABA: long-acting β-agonist; LAMA: long-acting muscarinic agonist; NA: not applicable; SABA: short-acting β_2-agonist.

Results

Exposure to CS sensitizes to elastin and elicits IL17A-predominant immune responses and bronchitis-like airway inflammation.

To investigate whether CS exposure sensitizes to elastin, mice were exposed to CS for two weeks followed by two weeks of rest prior to challenge with elastin on three consecutive days (**Fig. 1a**). Elastin challenge in CS-exposed mice induced significant neutrophilic airway inflammation, reaching up to 60% neutrophils in the bronchoalveolar lavage fluid (BALF) (**Fig. 1b**). Histological assessment showed neutrophilic airway inflammation, corroborating the observations in the BALF (**Fig. 1c)**. Neutrophilic inflammation was associated with increased expression of IL6, CXCL1, and CXCL2 in BALF (**Fig. 1d**). Neutrophilic inflammation elicited by elastin challenge in CS-exposed mice was dose dependent (**Supplementary Fig. 1**). While decreased, we observed significant neutrophilic airway inflammation and increased expression of CXCL1, CXCL2, and IL-6 following challenge with lower concentration of elastin. Of note, no inflammation was observed in mice exposed to CS and challenged with vehicle (normal saline) or mice challenged with elastin without prior exposure to CS (**Fig. 1b-d**). These findings indicate that inflammation was related to the combination of CS exposure and elastin administration, rather than inflammatory processes driven by elastin instillation alone or residual inflammation following two weeks of smoking cessation.

Flow cytometric analysis of lung T cells (**Supplementary Fig. 2**) showed that CS exposure followed by elastin challenge induced an IL17A-predominant T cell response (**Fig. 1e**), while no increase was observed in IFNγ positive T cells. Contrasting these observations, IFNγ and IL17A were both significantly elevated in lung tissues of CS exposed and elastin challenged mice (**Fig. 1f**). CS exposure and elastin challenge also induced a remarkable mucus hyperproduction, as evidenced by enhanced *Muc5ac* (mucin 5AC, oligomeric mucus/gel-forming) mRNA transcripts, Periodic acid–Schiff (PAS)-positive staining, and MUC5AC expression in the airway epithelium (**Fig. 1g-i**).

As a direct comparison, inflammatory parameters in the CS-elastin model were compared with the chronic CS exposure. CS exposure for 3 months induced airway inflammation, while all inflammatory markers were lower than those observed in the CS-elastin model (**Fig. 1b-i**). Collectively, these data demonstrate that CS exposure and elastin challenge induces a

bronchitis-like phenotype that appears more robust than chronic CS exposure alone.

Sensitization and short-term challenge with mouse elastin induce Th1 immune responses and a bronchitis-like airway inflammation in mice.

Elastin is a self-antigen; hence, it is plausible that a state of tolerance exists towards this antigen. To explore whether mice can be sensitized to elastin, mice were injected intraperitoneally with elastin and Freund's adjuvant followed by intratracheal challenge with elastin (**Supplementary Fig. 3a**). Elastin sensitization and challenge induced a bronchitis-like phenotype comparable to the CS-elastin model (**Supplementary Fig. 3b-i**) with the exception that the resulting T cell response was Th1-predominant (**Supplementary Fig. 3e**). Altogether, these data provide evidence that the CS-induced sensitization was likely targeted against elastin.

Cigarette smoke-sensitized T cell immunity facilitates mice to elastin-induced airway inflammation

Next, we investigated whether CS-induced sensitization to elastin persists for a prolonged period. To this end, mice were exposed to cigarette smoke and rested for 4, 12 and 24 weeks prior to intratracheal elastin challenge. Elastin challenge induced a significant neutrophilic airway inflammation at all time points, although levels of inflammation declined in a time-dependent manner (**Fig. 2a**). Assessment of lung histology and expression of CXCL1 showed increased inflammation at the 24-week time point (**Fig. 2b-c**). These data suggest that there might be T cell-mediated memory in CS-sensitized mice.

To show conclusively that inflammatory processes were T cell-dependent, we performed the following experiments. First, we transferred $CD3^+$ T cells from room air and CS-exposed mice into naïve recipients. Subsequently, recipient mice were challenged with elastin daily for 3 days. We observed a significant increase in neutrophilic airway inflammation and inflammatory mediators in mice that received T cells from CS-exposed mice (**Fig. 2d, e**). Of note, levels of Th17, rather than Tc17, Th1 or Tc1, were markedly elevated in mice adoptively transferred with T cells from cigarette smoke-exposed mice (**Fig. 2f**). Next, we exposed *Rag1*$^{-/-}$ mice to CS followed by elastin challenge. **Supplementary Fig. 4** shows that *Rag1*$^{-/-}$ are largely deficient of T cells. Of note, airway inflammation in the CS-elastin model was significantly attenuated in *Rag1*$^{-/-}$ mice

(**Fig. 2g, h**). We also isolated lung single-cell-suspensions from air control or CS-sensitized mice (with repeated CS exposure/rest cycle to intentionally enhance the T cell memory), and stimulated with elastin for 72 h. Although the levels of T cell response were very low (data not shown), while interestingly, the levels IL17A and IFNG in culture medium were significantly increased in the repeated CS exposure group (**Supplementary Fig. 5**). Together, these results suggested that the CS-exposure induced elastin-specific T cells that have the capability to drive autoimmune inflammatory processes.

IL17A mediates the airway inflammation induced by CS sensitization and elastin challenge

Since CS sensitization and elastin challenge induced IL17A-predominant T cell responses, we next investigated the role of IL17A in this model. All the bronchitis-like features induced by CS exposure and elastin challenge were significantly decreased in the *Il17a*$^{-/-}$ mice (**Fig. 3a-e**). Similarly, administration of an IL17A neutralizing monoclonal antibody during elastin challenge significantly attenuated neutrophilic airway inflammation in this model (**Fig. 3f**).

Taken together, these findings show that CS exposure sensitizes to elastin and that the inflammatory processes following exposure to elastin were IL17A-dependent.

MMP12 is critically required for CS-induced sensitization to elastin

To assess the CS-induced elastin specificity, CS-exposed mice were challenged with ovalbumin (OVA), an allergen commonly used for mouse model of asthma (**Fig. 4a**). Interestingly, OVA failed to induce airway inflammation in CS-exposed mice (**Fig. 4b**), suggesting that CS-induced sensitization was more specific to elastin.

We next aimed to explore the mechanisms that contribute to elastin sensitization in CS-exposed mice. The generation of elastin fragments in the lungs is generally attributed to neutrophil elastase (NE) and matrix metalloproteinases (MMPs) [13, 14], specifically, the macrophage metalloproteinase MMP12 [15, 16]. To test the function of NE, we exposed mice to lipopolysaccharide (LPS) (**Fig. 4a**), a well-known model of neutrophilic lung inflammation. Although LPS instillation induced a marked airway neutrophilia (**Fig. 4c**), elastin challenge following resolution of the initial inflammatory response did not induce neutrophilic airway inflammation in mice exposed to low dose LPS (**Fig. 4b**). These data suggest that LPS exposure is

less effective at eliciting elastin-specific immune responses compared to CS exposure.

To assess the function of MMP-12, we exposed *Mmp12*$^{-/-}$ mice to cigarette smoke followed by elastin challenge. In wild type mice, *Mmp12* mRNA expression was markedly increased in BALF cells of mice exposed to CS (**Fig. 4d**). Importantly, *Mmp12*$^{-/-}$ mice displayed markedly reduced neutrophilic inflammation in BALF and airways, decreased production of inflammatory cytokines, and diminished mucus production (**Fig. 4e-h**).

These data suggest that induction of MMP12 is critical for CS-induced sensitization to elastin, while neutrophils and neutrophil elastase play a less important role.

CS-induced elastin fragments drive the subsequent airway inflammation and mucus production

One of the pathologic mechanisms for MMP12 in COPD is due to the production of elastin fragments containing GXXPG or XGXPG conformational motives (where X is a hydrophobic amino acid) which exert a high monocyte chemotactic activity [17]. To investigate whether these motives contribute to inflammatory processes in the CS-elastin model, CS-exposed mice were challenged with peptides containing repeating VGVAPG sequences, a common and repeated motif in human elastin. VGVAPG peptides elicited a bronchitis-like phenotypes in CS-exposed mice (**Fig. 5a-e**).

We next treated mice with BA4 antibody during CS sensitization (**Fig. 5f**). This antibody has been shown to block the activity of endogenous elastin peptides, including the GXXPG and XGXPG motifs, and reduce the CS-induced airway inflammation in mice [17]. Neutrophilic airway inflammation following elastin challenge in CS-exposed mice was significantly attenuated by BA4 antibody treatment (**Fig. 5g-i**). Mucus hyperproduction induced by CS exposure and elastin challenge was also markedly reduced by BA4 (**Fig. 5j**).

These data suggest that the elastin fragments induced by CS exposure, most likely the GXXPG and XGXPG motifs, facilitate sensitization to elastin and orchestrate inflammatory responses and mucus hyperproduction in the CS-elastin model.

CS sensitization and sub-chronic elastin challenge induce an emphysema-like phenotype in mice

Next, we asked whether repeated elastin challenge in CS-exposed mice would elicit airway remodelling and airspace enlargement in mice, mimicking human emphysema. Mice were exposed to CS and then challenged with elastin every other day for 30 consecutive days (**Fig. 6a**). Repeated elastin challenge decreased the body weight (**Fig. 6b**) and induced a sustained neutrophilic airway inflammation (**Fig. 6c**). Persistent inflammation was associated with a marked decline in FEV_{20} and the FEV_{20}/FVC (**Fig. 6d**), increased the collagen deposition around airways (**Fig. 6e**) and evidence of mucus hyperproduction (**Fig. 6f**). Moreover, repeated elastin challenge led to a significant increase in lung airspace, as determined by comparative histologic examination and mean linear intercept (MLI) measurements (**Fig. 6g**). These data suggest that CS exposure and chronic elastin challenge induced a COPD-like phenotype similar to what is observed in mice exposed to CS for 6 months (**Supplementary Fig. 6**). It should be noted that in the chronic CS model, mice were generally 4 months older than those in the CS-elastin model. Though the levels of collagen deposition and the airspace enlargement were comparable between the two models, airway inflammation and mucus production induced by 6 months CS exposure appeared to be less severe compared to the CS-elastin model (**Supplementary Fig. 6** vs **Fig. 6**).

Elastin-mediated autoimmunity is elevated in COPD patients

Finally, we examined elastin-mediated immune responses in COPD patients (**Table 1**). In agreement with previous reports [6, 7], the levels of elastin antibodies in plasma were elevated in COPD patients (**Fig. 7a**). Moreover, levels of Th1, Th17, and Tc17 in peripheral blood were significantly increased in COPD patients relative to healthy controls (**Fig. 7b**). In induced sputum, protein levels of IL17A were increased (**Fig. 7c**). To address whether the pathogenic T cells in COPD could interact with elastin fragments, we selected an HLA-A*02:01 allele which presents a relatively high affinity to human elastin peptide GVAPGVGVAPGV to synthesize a tetramer. Peripheral blood mononuclear cells (PBMCs) from COPD patients with this allele exhibited significantly higher positive tetramer staining relative to those from healthy controls with the same allele (**Fig. 7d**). Taken together, these clinical data are in line with our observations in our animal studies, suggesting that elastin drives IL17A-predominant auto-immune processes in COPD.

Discussion

The nature of the molecular mechanisms that drive CS-induced airway inflammation remains a central question in COPD research. Building on previous reports that elastin may drive autoimmune processes in COPD [6, 7], we demonstrate that, in mice exposed to cigarette smoke, elastin serves as a self-antigen and drives adaptive immune responses that facilitates sensitization to subsequent elastin-induced COPD-like pathologies.

Recent evidence has suggested that elastin-mediated autoimmunity may be associated with COPD pathogenesis, as anti-elastin antibodies were present in patients with COPD [7], and elastin peptides could act as cognate antigens to stimulate Th1 and Th17 differentiation in subjects with emphysema [8]. Deslee *et al* observed an increase in elastin in very severe COPD patients [6]. In line with these observations, we found that antibodies against elastin were significantly elevated in COPD patients and that T cells from COPD patients bear T cell receptors that recognize elastin peptides. Moreover, we demonstrate that elastin sensitization and challenge induced the Th1-predominant immune response and subsequent bronchitis-like phenotypes, demonstrating that elastin, as a self-antigen, is able to elicit autoimmune responses in mice. Finally, CS-exposed mice were sensitized to elastin, providing experimental evidence that elastin-mediated autoimmunity may contribute to the pathogenesis of COPD. Gu et al have recently demonstrated that $CD4^+$ T cells from CS-exposed mice were reactive to elastin fragments *in vitro*, and that mice immunized with a combination of human and rat elastin fragments showed increased infiltration of innate and adaptive immune cells to the lungs and developed emphysema [18], completely in agreement with our conclusions.

Animal models currently used in COPD research have clear limitations, restricting their application to study the pathogenesis of COPD [19-21]. For example, models of CS-induced airspace enlargement are time-consuming, requiring in general 6 months of continuous CS exposure to induce emphysema formation. Airway inflammation in these models is mild (the proportion of neutrophils in BALF is usually less than 10%) and the mucus expression is rarely evident. Although protease instillation rapidly reproduces many characteristics of human emphysema, these models do not mimic a continuous inflammatory process and there is little evidence that T cell-driven processes are involved. This limits the application of elastase models for studying mechanisms of CS-induced airway inflammation and lung pathologies. The animal

model presented here overcomes these limitations. We observed moderate levels of neutrophilic airway inflammation (30-60% of neutrophils in BALF, comparable with proportions of eosinophils in asthma models), a Th1/Th17 inflammatory signature, marked mucus hyperproduction, increased airway remodelling, declined lung function, and enlarged airspaces. It required 1 month to establish airway inflammation, mimicking human bronchitis, and 2 months to establish parenchymal damage. In addition, our model provides "proof of concept" that autoimmune processes are induced by cigarette smoke exposure and may provide a novel framework for building animal models for other autoimmune diseases. This is of clinical relevance, as cigarette smoke exposure is a known risk factor for a number of autoimmune diseases, such as rheumatoid arthritis.

Airway mucus hypersecretion is one of the cardinal features for both COPD and asthma. However, unlike increased mucus hyperproduction in asthma models or by particulate matter [22-24], there is little evidence that CS exposure increases mucus production in mouse models. In contrast, acrolein, a reactive α, β-unsaturated aldehyde and component of cigarette smoke, readily induces mucus production in murine airways [25, 26]. Our findings identify elastin as an effective stimulator to trigger mucin expression in CS-exposed mice and, thus, provide a novel model for mucus research with relevance to COPD. In fact, we have observed that elastin peptides containing the active GXXPG conformational motif [27, 28], but not elastin protein, induced MUC5AC expression in human bronchial epithelial cells (data not shown), suggesting a critical role of these active peptides in driving mucus production in COPD.

Our current study emphasizes the pivotal role of MMP12 in initiating CS-induced autoimmune responses. In line with previous reports showing that *Mmp12*$^{-/-}$ mice are protected from CS-induced airway inflammation and emphysema [15], *Mmp12* deficiency markedly attenuated elastin-induced airway inflammation and mucus hyperproduction in mice with prior exposure to cigarette smoke. Other MMPs in *Mmp12*$^{-/-}$ alveolar macrophages were not altered (data not shown), and thus we could not rule out the functions of other MMPs in our study. In fact, MMP12 deficiency only partially attenuated inflammatory processes, supporting the participation of other MMPs in CS-induced autoimmunity. One of the mechanisms that implicates MMP12 in the pathogenesis of COPD is the production of elastin fragments that contain GXXPG or XGXPG motifs, which exert monocyte chemotactic activity [17]. In our current study, we found that

tetramers that contained elastin peptides with these motifs were able to directly bind T cells from COPD patients and induce airway inflammation in CS-sensitized mice. We further show that antibodies that target the active motif in elastin effectively attenuated airway inflammation when delivered during cigarette smoke exposure. Thus, the MMP12-generated elastin peptides induced by CS exposure not only are chemotactic factors for monocytes, but also initiate T cell responses, thereby driving subsequent airway inflammation, mucus production, and airspace enlargement.

It is noteworthy that COPD/emphysema generally develops decades after smoking cessation, accompanied by increased inflammation in patients' airways. These observations are consistent with our results in the murine model where mice developed airway inflammation following elastin challenge 6 months after an initial 2 weeks of CS exposure. Therefore, CS exposure may sensitize to elastin forming an immune memory that perpetuates inflammatory processes long after an individual quits smoking.

Accumulating evidence suggests that IL17A-driven immune processes may contribute to the pathogenesis of COPD, as increased levels of IL17A and elevated numbers of $IL17A^+$ cells have been detected in bronchial mucosa, peripheral blood, and sputum of COPD patients [29-31]. Similarly, we observed augmented concentration of IL17A in induced sputum and increased levels of Th17 and Tc17 in the blood of COPD patients. Moreover, animal studies have demonstrated that IL17A is increased in CS-induced airway injury [32-34] and *Il17a*$^{-/-}$ mice exposed to CS are protected from airspace enlargement [35, 36]. In line with these, IL17A was significantly increased in the elastin-driven airway inflammation in mice that were previously exposed to cigarette smoke. Genetic deficiency or neutralization of IL17A decreased elastin-driven inflammation, indicating a pivotal role of Th17/IL17A in the pathogenesis of COPD.

In conclusion, our findings demonstrate an elastin-mediated autoimmunity in CS exposed mice, which is orchestrated by upstream MMP12 and is mediated by the subsequent IL17A signalling. Based on this, we establish a novel mouse model mimicking most human COPD characteristics, and suggest that MMP12, active elastin peptides, or IL17A could serve as novel therapeutic targets for COPD.

Author contributions

J.S.Z., Z.Y.L., X.X.C., Y.Z., Y.W., H.P.C., Y.F.W., M.Z., J.L., L.L.D., N.X.X., T.W.L., C.Z., and Y.P.W., participated in data collection, analysis, and interpretation. C.H.D., H.Q.H., F.G.Y., W.H., Y.W., W.N.X., H.Q., T.C., D.W., H.P.L., F.L., and X.L. provided materials and technical support. X.B.Z., L.W., S.M.Y., W.L., M.E.C., M.S. participated in critical discussion of research design and review of the manuscript. J.S.Z., Z.Y.L., A.M.K.C., Z.H.C. and H.H.S. participated in the conception and design of the study and wrote the manuscript.

Acknowledgements

This work was supported by the Major Projects (2016YFA0501802 to Z.H.C.) from Ministry of Science & Technology, projects (81670031 to Z.H.C., 81930003 to H.H.S., and 8180010242 to J.S.Z.) from the National Natural Science Foundation of China, and project from US National Institutes of Health (R01 HL13219801 to M.E.C. and A.M.K.C., and R01 HL132198 to A.M.K.C.)

Conflict of interests

None declared.

Reference

1. Decramer M, Janssens W, Miravitlles M. Chronic obstructive pulmonary disease. *The Lancet* 2012: 379(9823): 1341-1351.
2. Hogg JC, Timens W. The pathology of chronic obstructive pulmonary disease. *Annu Rev Pathol* 2009: 4: 435-459.
3. Gamble E, Grootendorst DC, Hattotuwa K, O'Shaughnessy T, Ram FS, Qiu Y, Zhu J, Vignola AM, Kroegel C, Morell F, Pavord ID, Rabe KF, Jeffery PK, Barnes NC. Airway mucosal inflammation in COPD is similar in smokers and ex-smokers: a pooled analysis. *Eur Respir J* 2007: 30(3): 467-471.
4. Barnes PJ. Inflammatory mechanisms in patients with chronic obstructive pulmonary disease. *J Allergy Clin Immunol* 2016: 138(1): 16-27.
5. Brusselle GG, Joos GF, Bracke KR. New insights into the immunology of chronic obstructive pulmonary disease. *The Lancet* 2011: 378(9795): 1015-1026.
6. Deslee G, Woods JC, Moore CM, Liu L, Conradi SH, Milne M, Gierada DS, Pierce J, Patterson A, Lewit RA, Battaile JT, Holtzman MJ, Hogg JC, Pierce RA. Elastin expression in very severe human COPD. *Eur Respir J* 2009: 34(2): 324-331.
7. Lee SH, Goswami S, Grudo A, Song LZ, Bandi V, Goodnight-White S, Green L, Hacken-Bitar J, Huh J, Bakaeen F, Coxson HO, Cogswell S, Storness-Bliss C, Corry DB, Kheradmand F. Antielastin autoimmunity in tobacco smoking-induced emphysema. *Nat Med* 2007: 13(5): 567-569.
8. Shan M, Cheng HF, Song LZ, Roberts L, Green L, Hacken-Bitar J, Huh J, Bakaeen F, Coxson HO, Storness-Bliss C, Ramchandani M, Lee SH, Corry DB, Kheradmand F. Lung myeloid dendritic cells coordinately induce TH1 and TH17 responses in human emphysema. *Sci Transl Med* 2009: 1(4): 4ra10.
9. Cosio MG, Saetta M, Agusti A. Immunologic aspects of chronic obstructive pulmonary disease. *N Engl J Med* 2009: 360(23): 2445-2454.
10. Cottin V, Fabien N, Khouatra C, Moreira A, Cordier JF. Anti-elastin autoantibodies are not present in combined pulmonary fibrosis and emphysema. *Eur Respir J* 2009: 33(1): 219-221.
11. Greene CM, Low TB, O'Neill SJ, McElvaney NG. Anti-proline-glycine-proline or antielastin autoantibodies are not evident in chronic inflammatory lung disease. *Am J Respir Crit Care Med* 2010: 181(1): 31-35.
12. GOLD Committee. Global strategy for the diagnosis, management, and prevention of COPD. 2017 [cited May 3, 2017]; Available from: http://www.goldcopd.org/guidelines-pocket-guide-to-copd-diagnosis.html
13. Churg A, Zhou S, Wright JL. Series "matrix metalloproteinases in lung health and disease": Matrix metalloproteinases in COPD. *Eur Respir J* 2012: 39(1): 197-209.
14. Elkington PT, Friedland JS. Matrix metalloproteinases in destructive pulmonary pathology. *Thorax* 2006: 61(3): 259-266.
15. Hautamaki RD, Kobayashi DK, Senior RM, Shapiro SD. Requirement for macrophage elastase for cigarette smoke-induced emphysema in mice. *Science* 1997: 277(5334): 2002-2004.
16. Hunninghake GM, Cho MH, Tesfaigzi Y, Soto-Quiros ME, Avila L, Lasky-Su J, Stidley C, Melen E, Soderhall C, Hallberg J, Kull I, Kere J, Svartengren M, Pershagen G, Wickman M, Lange C, Demeo DL, Hersh CP, Klanderman BJ, Raby BA, Sparrow D, Shapiro SD, Silverman EK, Litonjua AA, Weiss ST, Celedon JC. MMP12, lung function, and COPD in high-risk populations. *N Engl J Med* 2009: 361(27): 2599-2608.
17. Houghton AM, Quintero PA, Perkins DL, Kobayashi DK, Kelley DG, Marconcini LA, Mecham RP,

Senior RM, Shapiro SD. Elastin fragments drive disease progression in a murine model of emphysema. *J Clin Invest* 2006: 116(3): 753-759.

18. Gu BH, Sprouse ML, Madison MC, Hong MJ, Yuan X, Tung HY, Landers CT, Song LZ, Corry DB, Bettini M, Kheradmand F. A Novel Animal Model of Emphysema Induced by Anti-Elastin Autoimmunity. *J Immunol*. 2019: 203(2): 349-359.

19. Shapiro SD. Animal models for COPD. *Chest* 2000: 117(5 Suppl 1): 223s-227s.

20. Vlahos R, Bozinovski S. Preclinical murine models of Chronic Obstructive Pulmonary Disease. *Eur J Pharmacol* 2015: 759: 265-271.

21. Wright JL, Cosio M, Churg A. Animal models of chronic obstructive pulmonary disease. *Am J Physiol Lung Cell Mol Physiol* 2008: 295(1): L1-L15.

22. Lai T, Wu M, Zhang C, Che L, Xu F, Wang Y, Wu Y, Xuan N, Cao C, Du X, Wu B, Li W, Ying S, Shen H, Chen Z. HDAC2 attenuates airway inflammation by suppressing IL-17A production in HDM-challenged mice. *Am J Physiol Lung Cell Mol Physiol.* 2019: 316(1): L269-L279.

23. Qin XJ, Zhang GS, Zhang X, Qiu ZW, Wang PL, Li YW, Li W, Xie QM, Ke YH, Lee JJ, Shen HH. Protein tyrosine phosphatase SHP2 regulates TGF-beta1 production in airway epithelia and asthmatic airway remodeling in mice. *Allergy* 2012: 67(12): 1547-1556.

24. Chen ZH, Wu YF, Wang PL, Wu YP, Li ZY, Zhao Y, Zhou JS, Zhu C, Cao C, Mao YY, Xu F, Wang BB, Cormier SA, Ying SM, Li W, Shen HH. Autophagy is essential for ultrafine particle-induced inflammation and mucus hyperproduction in airway epithelium. *Autophagy* 2016: 12(2):297-311.

25. Deshmukh HS, McLachlan A, Atkinson JJ, Hardie WD, Korfhagen TR, Dietsch M, Liu Y, Di PY, Wesselkamper SC, Borchers MT, Leikauf GD. Matrix metalloproteinase-14 mediates a phenotypic shift in the airways to increase mucin production. *Am J Respir Crit Care Med* 2009: 180(9): 834-845.

26. Wang T, Liu Y, Chen L, Wang X, Hu XR, Feng YL, Liu DS, Xu D, Duan YP, Lin J, Ou XM, Wen FQ. Effect of sildenafil on acrolein-induced airway inflammation and mucus production in rats. *Eur Respir J* 2009: 33(5): 1122-1132.

27. Meghraoui-Kheddar A, Pierre A, Sellami M, Audonnet S, Lemaire F, Le Naour R. Elastin receptor (S-gal) occupancy by elastin peptides modulates T-cell response during murine emphysema. *Am J Physiol Lung Cell Mol Physiol* 2017: 313(3): L534-L547.

28. Sellami M, Meghraoui-Kheddar A, Terryn C, Fichel C, Bouland N, Diebold MD, Guenounou M, Hery-Huynh S, Le Naour R. Induction and regulation of murine emphysema by elastin peptides. *Am J Physiol Lung Cell Mol Physiol* 2016: 310(1): L8-23.

29. Doe C, Bafadhel M, Siddiqui S, Desai D, Mistry V, Rugman P, McCormick M, Woods J, May R, Sleeman MA, Anderson IK, Brightling CE. Expression of the T helper 17-associated cytokines IL-17A and IL-17F in asthma and COPD. *Chest* 2010: 138(5): 1140-1147.

30. Vanaudenaerde BM, Verleden SE, Vos R, De Vleeschauwer SI, Willems-Widyastuti A, Geenens R, Van Raemdonck DE, Dupont LJ, Verbeken EK, Meyts I. Innate and adaptive interleukin-17-producing lymphocytes in chronic inflammatory lung disorders. *Am J Respir Crit Care Med* 2011: 183(8): 977-986.

31. Lai T, Tian B, Cao C, Hu Y, Zhou J, Wang Y, Wu Y, Li Z, Xu X, Zhang M, Xu F, Cao Y, Chen M, Wu D, Wu B, Dong C, Li W, Ying S, Chen Z, Shen H. HDAC2 Suppresses IL17A-Mediated Airway Remodeling in Human and Experimental Modeling of COPD. *Chest* 2018: 153(4): 863-875.

32. Geraghty P, Hardigan A, Foronjy RF. Cigarette smoke activates the proto-oncogene c-src to promote airway inflammation and lung tissue destruction. *Am J Respir Cell Mol Biol* 2014: 50(3):

559-570.
33. Harrison OJ, Foley J, Bolognese BJ, Long E, 3rd, Podolin PL, Walsh PT. Airway infiltration of CD4+ CCR6+ Th17 type cells associated with chronic cigarette smoke induced airspace enlargement. *Immunol Lett* 2008: 121(1): 13-21.
34. Zhou H, Hua W, Jin Y, Zhang C, Che L, Xia L, Zhou J, Chen Z, Li W, Shen H. Tc17 cells are associated with cigarette smoke-induced lung inflammation and emphysema. *Respirology* 2015: 20(3): 426-433.
35. Shan M, Yuan X, Song LZ, Roberts L, Zarinkamar N, Seryshev A, Zhang Y, Hilsenbeck S, Chang SH, Dong C, Corry DB, Kheradmand F. Cigarette smoke induction of osteopontin (SPP1) mediates T(H)17 inflammation in human and experimental emphysema. *Sci Transl Med* 2012: 4(117): 117ra119.
36. Voss M, Wolf L, Kamyschnikow A, Wonnenberg B, Honecker A, Herr C, Lepper PM, Wegmann M, Menger MD, Bals R, Beisswenger C. Il-17A contributes to maintenance of pulmonary homeostasis in a murine model of cigarette smoke-induced emphysema. *Am J Physiol Lung Cell Mol Physiol* 2015: 309(2): L188-195.

Figure Legends

Figure 1. Exposure to CS sensitizes to elastin and elicits IL17A-predominant immune responses and bronchitis-like airway inflammation. (a) Experimental outline. Mice were exposed to CS or room air for 2 weeks, and were hosted at room air for another 2 weeks. Mice were then challenged with elastin (Eln, 100 μg) or normal saline (NS) intratracheally (i.t.) for 3 times at day 29, 30, and 31, and were sacrificed 48 h after the last elastin challenge. For the traditional CS model, mice were exposed to CS for 3 months, as detailed in Materials and Methods. **(b)** Inflammatory cell counts in the BALF. **(c)** Representative images and semi-quantified scoring of H&E staining of mouse lung sections. **(d)** The concentrations of CXCL1, CXCL2, and IL6 in BALF. **(e)** Levels of Th1, Tc1, Th17, and Tc17 in mouse lungs. **(f)** Levels of IFNG and IL17A in mouse lung homogenates. **(g)** Expression of *Muc5ac* mRNA transcripts in mouse lungs. **(h,i)** Representative images and the semi-quantified scorings of PAS **(h)** or MUC5AC **(i)** staining in mouse lung sections. Labelling for all the columns throughout Fig. 1 was shown in Fig. 1b. Mac: macrophages; Neu: neutrophils; Lym: lymphocytes; Eos: eosinophils. Throughout, data are representative of 5-6 mice and were replicated in at least 3 independent experiments. Data are mean ± s.e.m. *P < 0.05, **P < 0.01, ***P < 0.001 by one-way ANOVA. n.s., not significant.

Figure 2. Cigarette smoke-sensitized T cell immunity facilitates mice to elastin-induced airway inflammation. (**a-c**) Mice were exposed to CS for 2 weeks, and seated at room air for 4, 12, or 24 weeks. Mice were then challenged with elastin (Eln, 100 μg) intratracheally (i.t.) once a day for 3 days and were sacrificed 48 h after the last elastin challenge. **(a)** Total inflammatory cell and neutrophil counts in the BALF. **(b)** Representative images of H&E staining and the semi-quantified scoring of mouse lung sections. **(c)** Concentrations of CXCL1 in BALF (left panel) and lung tissues (right panel). (**d-f**) $CD3^+$ T cells from mediastinal lymph nodes of air controls or CS-sensitized mice were transferred to naïve recipients and were challenged with elastin, and the inflammatory cell counts **(d)**, inflammatory factors of CXCL1, CXCL2 and IL6 in BALF **(e)** and T cell responses in lung **(f)** were detected. **(g-h)** *Rag1*$^{-/-}$ attenuated the airway inflammation induced by CS-sensitization

and elastin challenge. **(g)** Inflammatory cells in BALF. **(h)** The concentrations of CXCL1, CXCL2, and IL6 in BALF. Mac: macrophages; Neu: neutrophils; Lym: lymphocytes; Eos: eosinophils. Throughout, data are representative of 3-6 mice. Data are mean ± s.e.m. *P < 0.05, **P < 0.01, ***P < 0.001 by one-way ANOVA.

Figure 3. IL17A mediates the airway inflammation induced by CS sensitization and elastin challenge

Il17a$^{-/-}$ mice and wildtype controls (WT) were sensitized with CS and challenged with elastin, and the inflammatory cell counts in BALF **(a)**, H&E staining and the semi-quantified inflammatory scoring **(b),** the concentrations of CXCL1, CXCL2, and IL6 in BALF **(c)**, the expression of *Muc5ac* in lung tissues **(d)**, and the mucus hyperproduction in airways **(e)** were detected. (**f**) IL17A neutralization attenuates the inflammatory cell counts in BALF. IL17A neutralization antibody (5 μg) was administrated intratracheally together with elastin challenge. Mac: macrophages; Neu: neutrophils; Lym: lymphocytes; Eos: eosinophils. Throughout, data are representative of 3-6 mice. Data are mean ± s.e.m. **P < 0.01, ***P < 0.001 by one-way ANOVA.

Figure 4. MMP12 is critically required for CS-induced sensitization to elastin. (a) Experimental outline. Mice were sensitized with intratracheal instillation of LPS (1 μg per mouse) at day 0 and 14, or 2 weeks of CS exposure. Mice were then challenged with elastin or ovalbumin (OVA) for 3 times at indicated time points. **(b)** Inflammatory cell counts in the BALF. **(c)** Time course of the amounts of neutrophils or macrophages in BALF intratracheally treated with LPS (1 μg for twice) or exposed to CS for 2 weeks. **(d)** The levels of *Mmp12* mRNA transcripts in BALF cells from mice sensitized with CS for 2 weeks, or elastin plus CFA. **(e-h)** *Mmp12*$^{-/-}$ mice and wildtype controls (WT) were sensitized with CS and challenged with elastin, and the inflammatory cell counts in BALF **(e)**, H&E staining and the semi-quantified inflammatory scoring **(f),** the concentrations of CXCL1, CXCL2, and IL6 in BALF **(g)**, and the mucus hyperproduction in airways **(h)** were detected. Mac: macrophages; Neu: neutrophils; Lym: lymphocytes; Eos: eosinophils. Throughout, data are representative of 5-6 mice and were replicated in at least 3 independent experiments. Data are mean ± s.e.m. *P

< 0.05, **P < 0.01, ***P < 0.001 by student's t-test (**a-c**, for comparisons of two groups) or by one-way ANOVA (**d,f**,**g**, for comparisons of multiple groups).

Figure 5. CS-induced elastin fragments drive the subsequent airway inflammation and mucus production. (a-e) Airway inflammation induced by elastin peptides containing repeated VGVAPG. Experimental protocol was as shown in Fig. 1a, except using elastin peptides for challenge instead of elastin protein. **(a)** Inflammatory cell counts in the BALF. **(b)** Representative images and semi-quantified scoring of H&E staining of mouse lung sections. **(c)** The concentrations of CXCL1 and IL6 in BALF. **(d)** Expression of *Muc5ac* mRNA transcripts in mouse lungs. **(e)** Representative images and the semi-quantified scorings of PAS staining in mouse lung sections. **(f)** Protocol for BA4 antibody treatment. BA4 antibody (10 μg) was administrated intratracheally 1 h before everyday CS exposure. **(g-j)** BA4 attenuated the airway inflammation induced by CS-sensitization and elastin challenge. **(g)** Inflammatory cells in BALF. **(h)** Representative images and semi-quantified scoring of H&E staining of mouse lung sections. **(i)** The concentrations of CXCL2 and IL6 in BALF. **(j)** Representative images and the semi-quantified scorings of PAS staining in mouse lung sections. Mac: macrophages; Neu: neutrophils; Lym: lymphocytes; Eos: eosinophils. Throughout, data are representative of 5-6 mice and were replicated in at least 3 independent experiments. Data are mean ± s.e.m. **P < 0.01, ***P < 0.001 by one-way ANOVA.

Figure 6. CS sensitization and sub-chronic elastin challenge induce an emphysema-like phenotype in mice. (a) Experimental outline. Mice were exposed to CS or room air for 2 weeks and were hosted at room air for another 2 weeks. Mice were then challenged with elastin (Eln, 100 μg) or normal saline (NS) intratracheally (i.t.) every other day for 30 days, and were sacrificed 48 h after the last elastin challenge. (**b**) Mouse weight at indicated time points. **(c)** Inflammatory cell counts in the BALF. **(d)** Lung function of mice sub-chronically challenged with elastin (n=14). Representative images of Masson's trichrome staining **(e)** and PAS staining **(f)** of mouse lung sections and the semi-quantified scoring. **(g)** Representative images of airspace and measurement of the mean linear intercept (MLI) of mouse lungs (n=10-16). Mac: macrophages; Neu: neutrophils; Lym: lymphocytes; Eos: eosinophils. FEV_{20}:

forced expiratory volume in 20 seconds; FVC: forced vital capacity. Throughout, data are representative of 6-8 mice unless otherwise indicated, and were replicated in at least 3 independent experiments. Data are mean ± s.e.m. *P < 0.05, **P < 0.01, ***P < 0.001 by student's t-test.

Figure 7. Elastin-mediated autoimmunity is elevated in COPD patients. (a) Expression of elastin antibody in plasma of COPD patients or healthy controls. The clinical information of human subjects was shown inf Supplementary Table 1. **(b)** Levels of Th1, Tc1, Th17, and Tc17 in peripheral blood from healthy controls (n=20) or patients with COPD (n=17). **(c)** Levels of IL17A in induced sputum from healthy controls and COPD patients. **(d)** Increased levels of elastin-specific T cells in COPD. PBMCs were collected from human subjects with HLA-A*02:01 genotype (n=3 for either group) and were cultured in the presence of IL2 for 7 d. Cells were then stained with specific tetramer bearing human elastin peptide GVAPGVGVAPGV and were analysed by flow cytometry. Representative images of tetramer staining and quantified results were shown. Data are mean ± s.e.m. *P < 0.05, **P < 0.01, ***P < 0.001, n.s., not significant, by student's t-test.

Figure 1

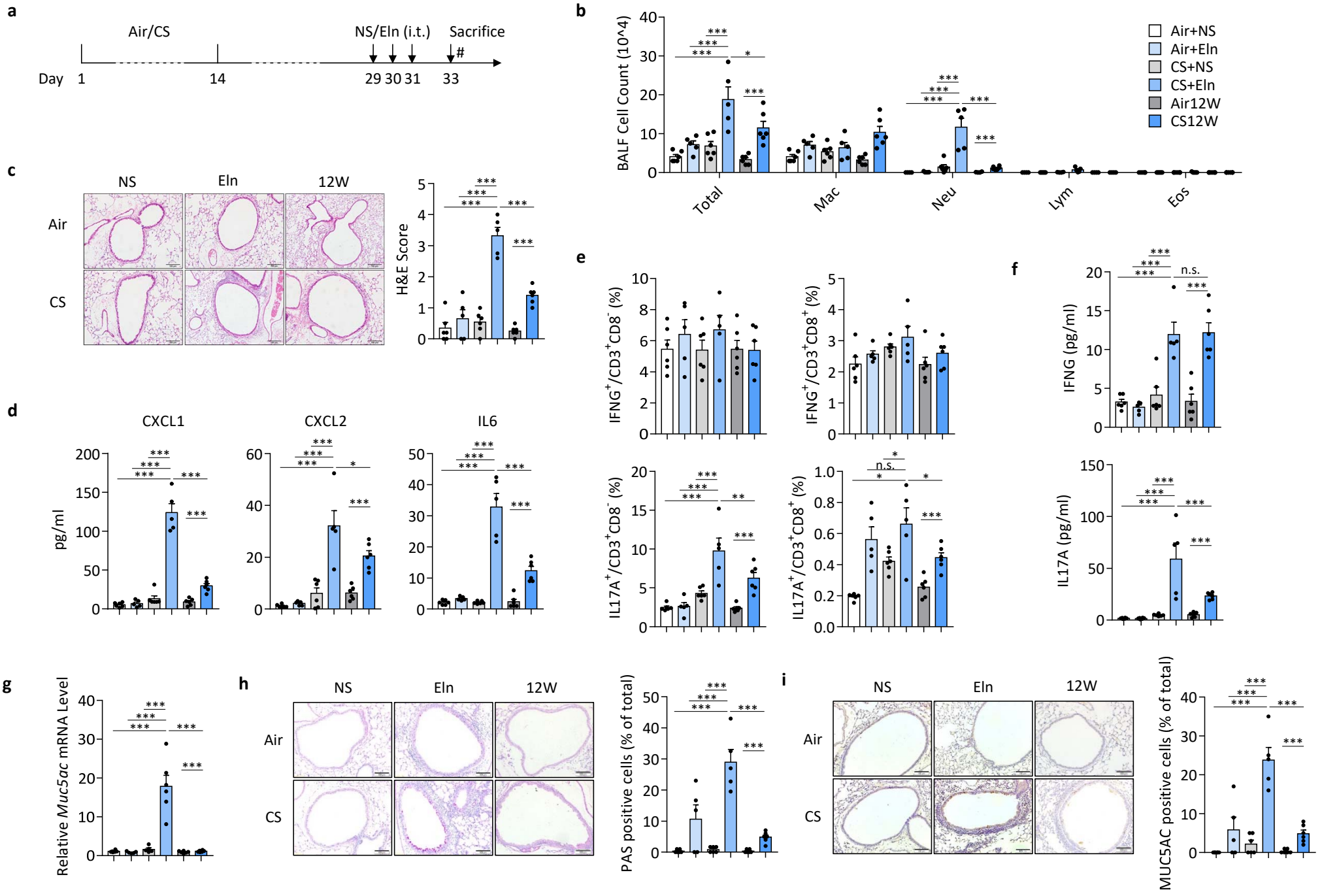
a
Air/CS
NS/Eln (i.t.)
Sacrifice
Day 1 14 29 30 31 33
b
BALF Cell Count (10^4)
Total
Mac
Neu
Lym
Eos
Air+NS
Air+Eln
CS+NS
CS+Eln
Air12W
CS12W
c
NS
Eln
12W
Air
CS
H&E Score
d
CXCL1
CXCL2
IL6
pg/ml
e
IFNG+/CD3+CD8- (%)
IFNG+/CD3+CD8+ (%)
IL17A+/CD3+CD8- (%)
IL17A+/CD3+CD8+ (%)
f
IFNG (pg/ml)
IL17A (pg/ml)
n.s.
g
Relative Muc5ac mRNA Level
h
PAS positive cells (% of total)
i
MUC5AC positive cells (% of total)

Figure 2

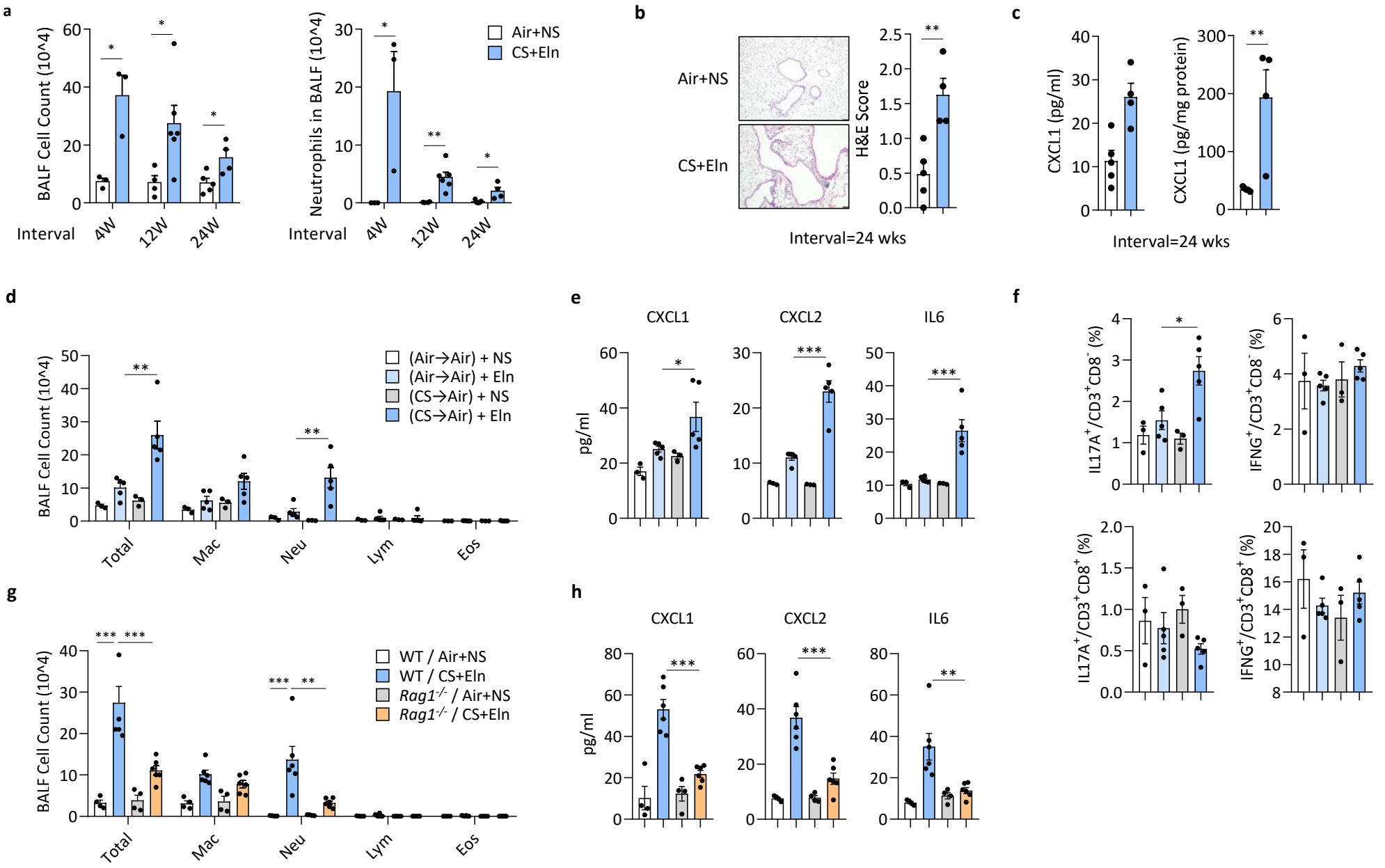
a
BALF Cell Count (10^4)
Neutrophils in BALF (10^4)
Air+NS
CS+Eln
Interval
4W
12W
24W
b
Air+NS
CS+Eln
H&E Score
Interval=24 wks
c
CXCL1 (pg/ml)
CXCL1 (pg/mg protein)
Interval=24 wks
d
BALF Cell Count (10^4)
(Air→Air) + NS
(Air→Air) + Eln
(CS→Air) + NS
(CS→Air) + Eln
Total
Mac
Neu
Lym
Eos
e
CXCL1
CXCL2
IL6
pg/ml
f
IL17A+/CD3+CD8- (%)
IFNG+/CD3+CD8- (%)
IL17A+/CD3+CD8+ (%)
IFNG+/CD3+CD8+ (%)
g
BALF Cell Count (10^4)
WT / Air+NS
WT / CS+Eln
Rag1-/- / Air+NS
Rag1-/- / CS+Eln
Total
Mac
Neu
Lym
Eos
h
CXCL1
CXCL2
IL6
pg/ml

Figure 3

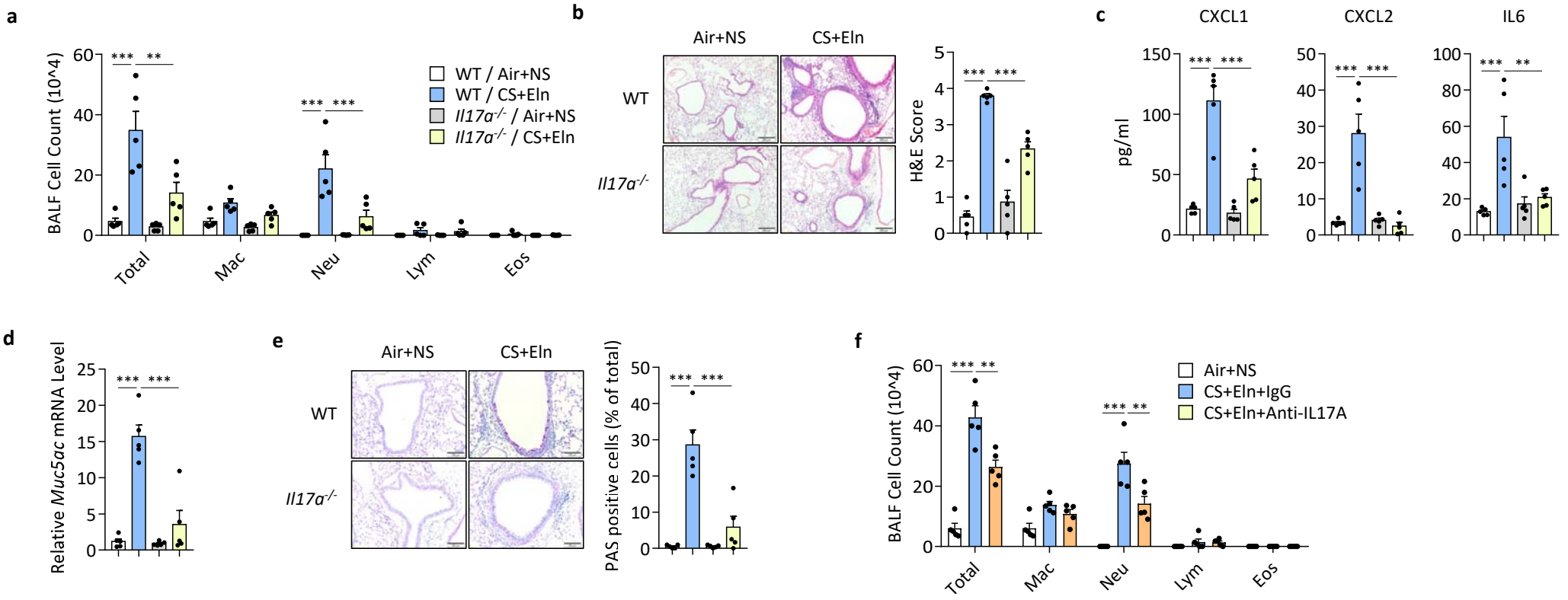
a
BALF Cell Count (10^4)
WT / Air+NS
WT / CS+Eln
Il17a-/- / Air+NS
Il17a-/- / CS+Eln
Total
Mac
Neu
Lym
Eos
b
Air+NS
CS+Eln
WT
Il17a-/-
H&E Score
c
CXCL1
CXCL2
IL6
pg/ml
d
Relative Muc5ac mRNA Level
e
PAS positive cells (% of total)
f
Air+NS
CS+Eln+IgG
CS+Eln+Anti-IL17A

Figure 4

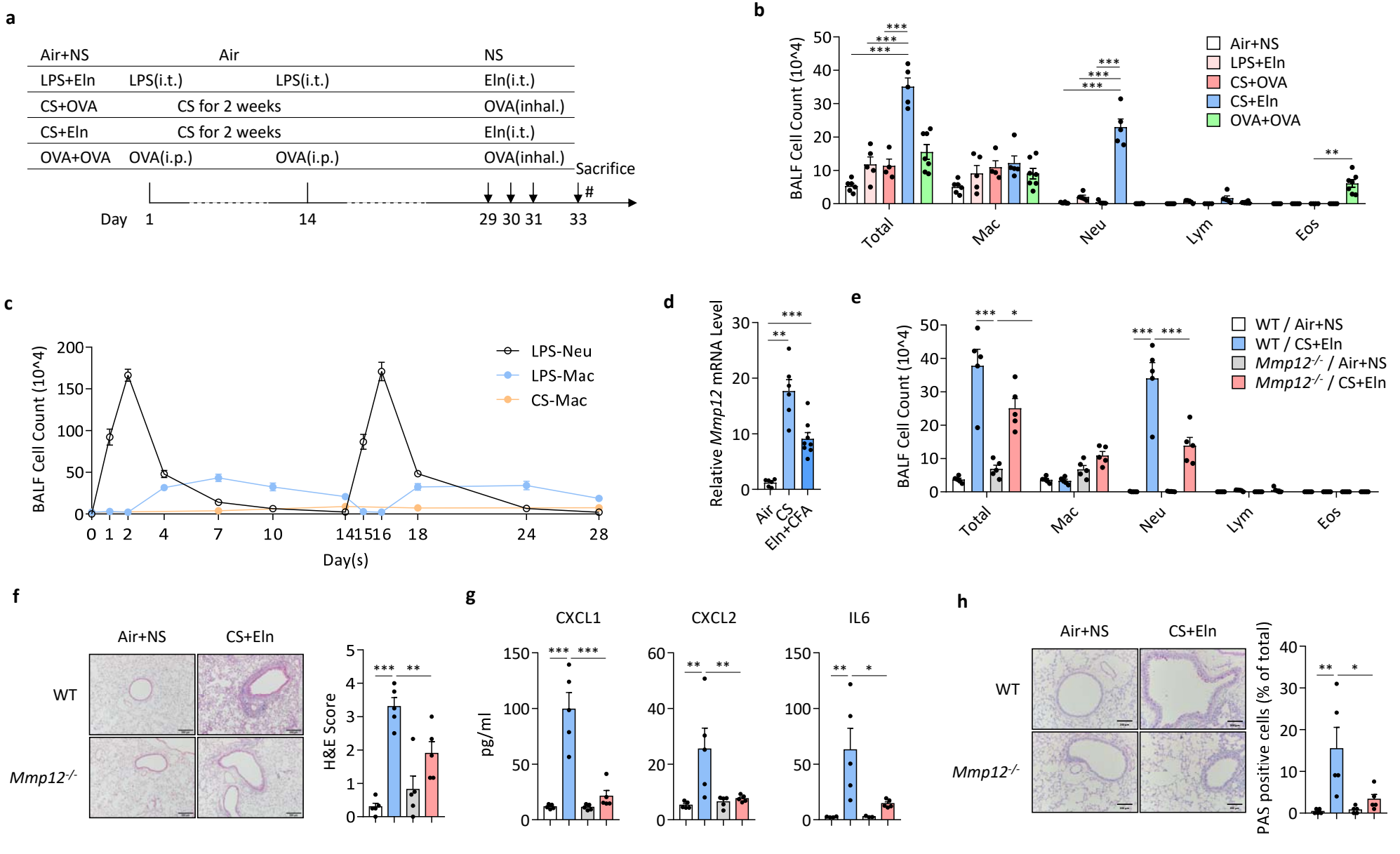
a
Air+NS Air NS
LPS+Eln LPS(i.t.) LPS(i.t.) Eln(i.t.)
CS+OVA CS for 2 weeks OVA(inhal.)
CS+Eln CS for 2 weeks Eln(i.t.)
OVA+OVA OVA(i.p.) OVA(i.p.) OVA(inhal.)
Sacrifice
Day 1 14 29 30 31 33
b
BALF Cell Count (10^4)
Air+NS
LPS+Eln
CS+OVA
CS+Eln
OVA+OVA
Total Mac Neu Lym Eos
c
BALF Cell Count (10^4)
LPS-Neu
LPS-Mac
CS-Mac
Day(s)
d
Relative Mmp12 mRNA Level
Air CS Eln+CFA
e
BALF Cell Count (10^4)
WT / Air+NS
WT / CS+Eln
Mmp12-/- / Air+NS
Mmp12-/- / CS+Eln
Total Mac Neu Lym Eos
f
Air+NS CS+Eln
WT
Mmp12-/-
H&E Score
g
CXCL1 CXCL2 IL6
pg/ml
h
Air+NS CS+Eln
WT
Mmp12-/-
PAS positive cells (% of total)

Figure 5

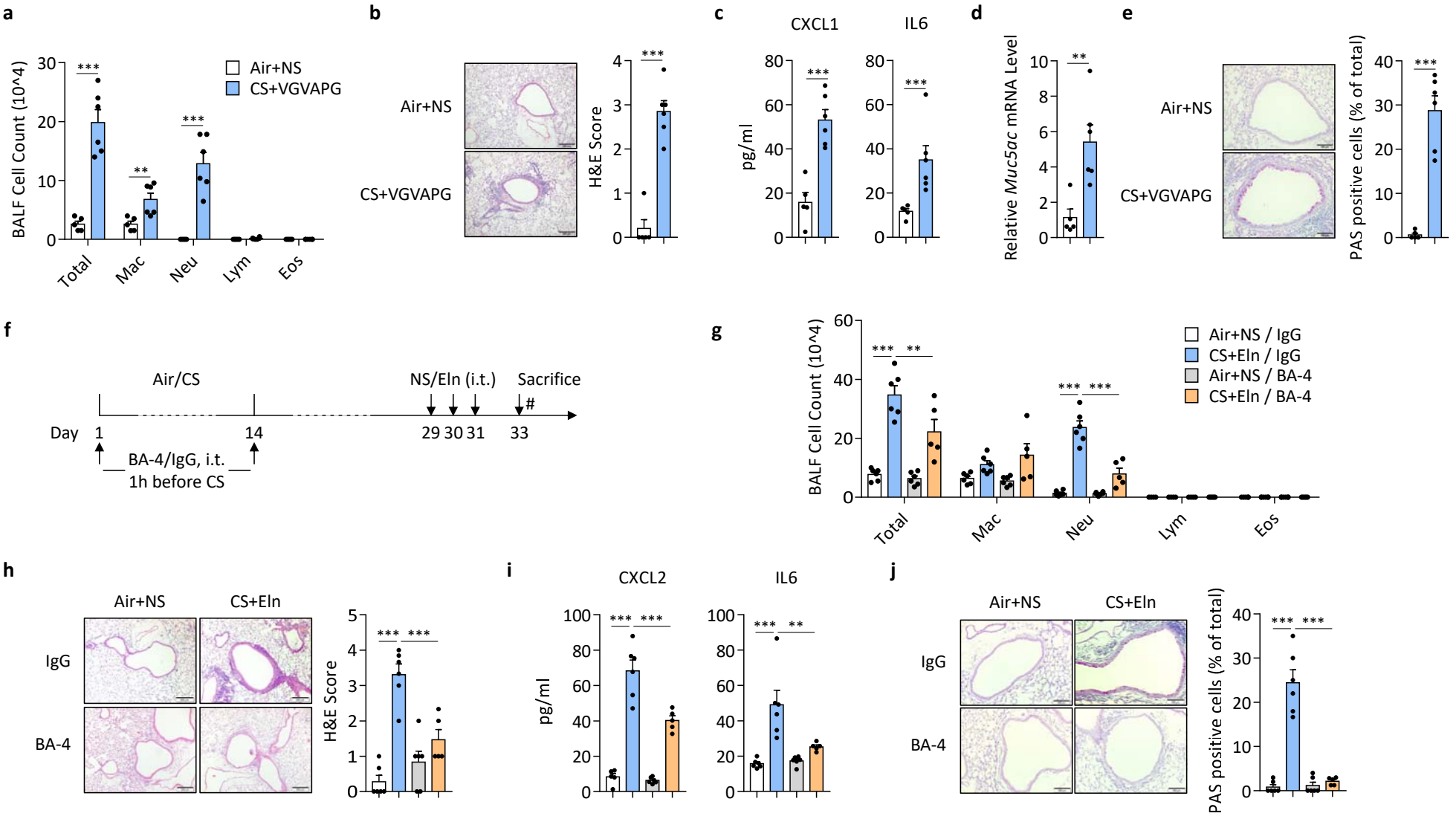
a
BALF Cell Count (10^4)
Air+NS
CS+VGVAPG
Total
Mac
Neu
Lym
Eos
b
Air+NS
CS+VGVAPG
H&E Score
c
CXCL1
IL6
pg/ml
d
Relative Muc5ac mRNA Level
e
Air+NS
CS+VGVAPG
PAS positive cells (% of total)
f
Air/CS
NS/Eln (i.t.)
Sacrifice
Day 1
14
29 30 31
33
BA-4/IgG, i.t.
1h before CS
g
BALF Cell Count (10^4)
Air+NS / IgG
CS+Eln / IgG
Air+NS / BA-4
CS+Eln / BA-4
Total
Mac
Neu
Lym
Eos
h
Air+NS
CS+Eln
IgG
BA-4
H&E Score
i
CXCL2
IL6
pg/ml
j
Air+NS
CS+Eln
IgG
BA-4
PAS positive cells (% of total)

Figure 6

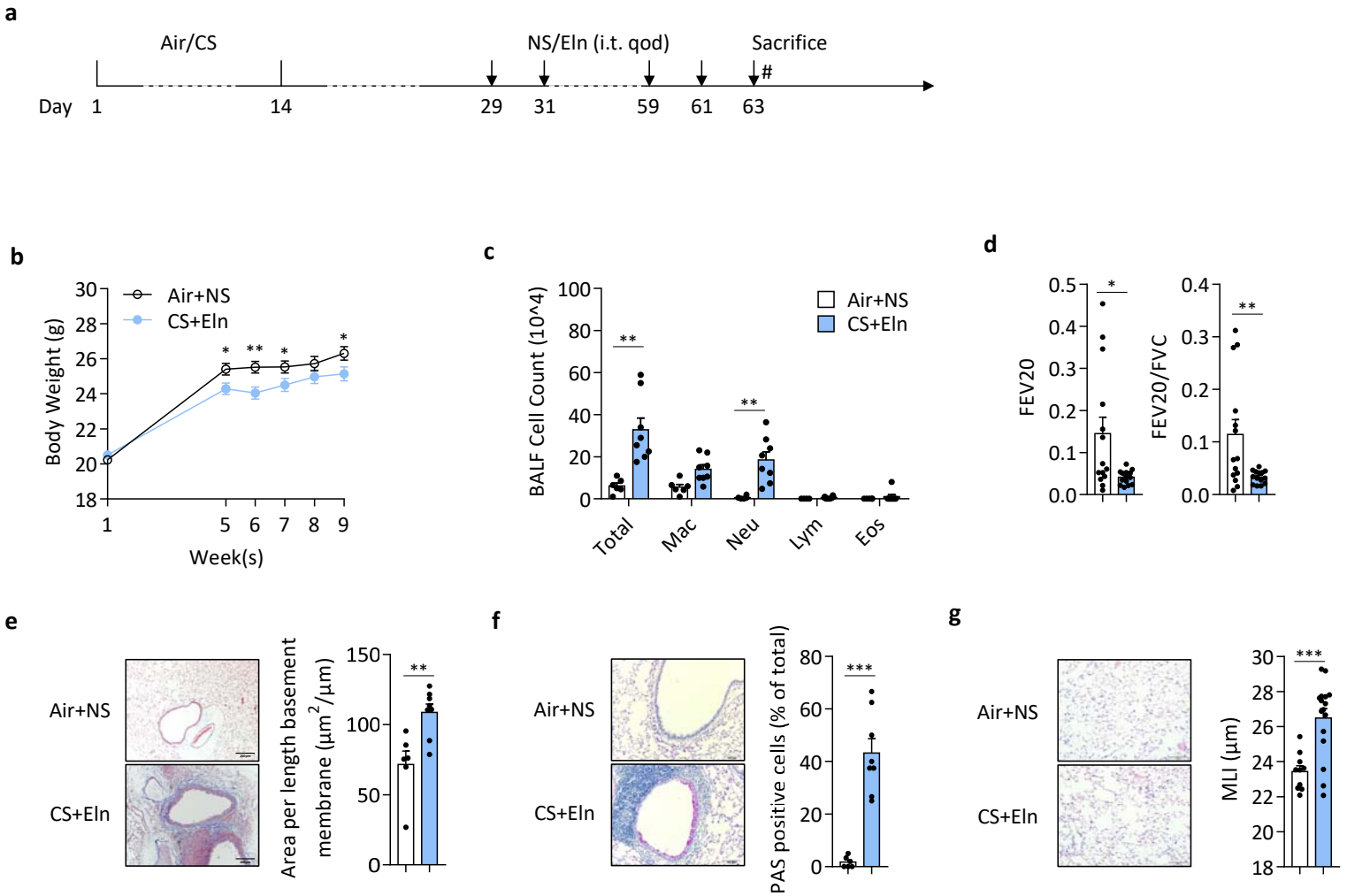
a
Air/CS
NS/Eln (i.t. qod)
Sacrifice
#
Day 1 14 29 31 59 61 63
b
Air+NS
CS+Eln
Body Weight (g)
Week(s)
c
BALF Cell Count (10^4)
Total
Mac
Neu
Lym
Eos
d
FEV20
FEV20/FVC
e
Air+NS
CS+Eln
Area per length basement membrane (μm²/μm)
f
PAS positive cells (% of total)
g
MLI (μm)

Figure 7

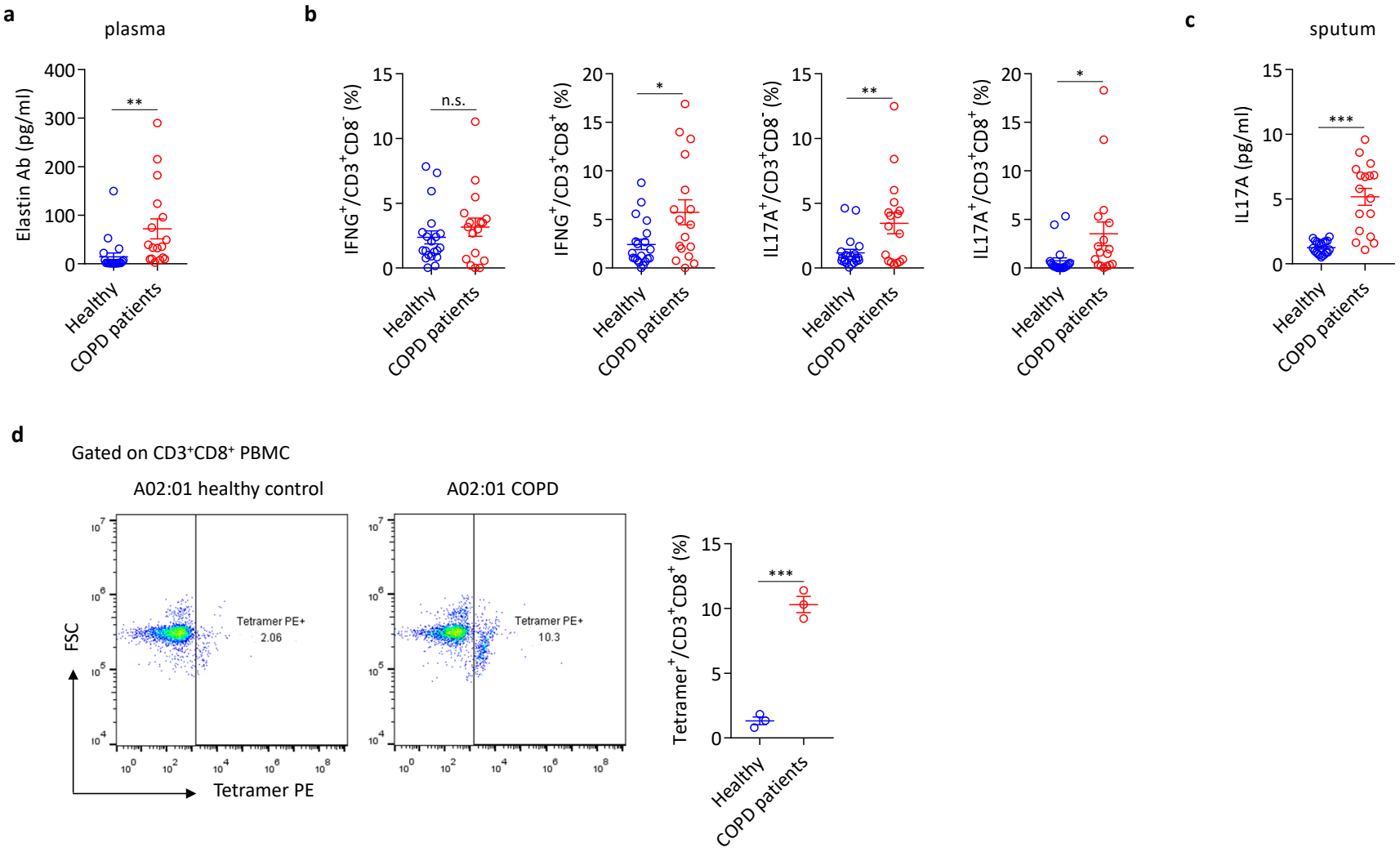
a
plasma
Elastin Ab (pg/ml)
400
300
200
100
0
**
Healthy
COPD patients
b
IFNG+/CD3+CD8- (%)
15
10
5
0
n.s.
IFNG+/CD3+CD8+ (%)
20
15
10
5
0
*
IL17A+/CD3+CD8- (%)
15
10
5
0
**
IL17A+/CD3+CD8+ (%)
20
15
10
5
0
*
Healthy
COPD patients
c
sputum
IL17A (pg/ml)
15
10
5
0
***
Healthy
COPD patients
d
Gated on CD3+CD8+ PBMC
A02:01 healthy control
A02:01 COPD
FSC
Tetramer PE
Tetramer PE+
2.06
Tetramer PE+
10.3
Tetramer+/CD3+CD8+ (%)
15
10
5
0
***
Healthy
COPD patients

Online Data Supplement

METHODS

$CD3^+$ T cell isolation and transfer

Mouse mediastinal lymph nodes from air- or CS- sensitised C57BL/6 mice were harvested after euthanasia, and single-cell suspensions were prepared using sterile syringe plunger. Cells were finally strained through a 40-mm filter. $CD3^+$ T cells were purified with Mojosort™ mouse CD3 T cell isolation kit (Biolegend, 480024) according to the manufacturer's protocol and were delivered ($1x10^6$ cells/mouse) intratracheally in 50 μl PBS to naïve recipient under anaesthesia. Recipient mice were challenged one day after T cell transfer with 50 μg elastin per day for 3 days.

BALF collection

Forty-eight hours after the last exposure to elastin, mice were sacrificed using an overdose of 2% pentobarbital sodium and tracheotomy was performed. Each mouse was lavaged with 0.4 ml PBS by injecting into the lungs and drawing to collect cells for 3 times. The total number of BALF cells was counted, then the remaining BALF was centrifuged (400 g for 10min at 4℃). The supernatant was retained for further analysis, while the cell pellet was resuspended in PBS moderately and centrifuged on glass slides. Then cells on glass slides were stained with Wright–Giemsa stain (Baso, BA-4017), and differential counts were assessed by counting 200 total cells.

Quantitative real-time PCR

RNA from BALF cells and lung homogenates was isolated with Trizol (Invitrogen, 15596026). Reverse transcription was performed with Reverse Transcription Reagents (Takara Biotechnology, DRR037A). Real-time RT-PCR was performed using the StepOnePlus PCR system and gene expression assays (Applied Biosystems, Foster City, CA, USA). A ΔΔCt method was used to quantify mRNA levels for *Muc5ac* and *Mmp12*. Gene expression was quantified using ABI and MS Excel software. Each sample was assayed in

triplicate. PCR primers used are shown as below: (Mouse *Gapdh*: Forword: 5'-AGGTCGGTGTGAACGGATTTG-3', Reverse: 5'-GGGGTCGTTGATGGCAACA-3'; Mouse *Muc5ac*: Forword: 5'-CTGTGACATTATCCCATAAGCCC-3', Reverse: 5'-AAGGGGTATAGCTGGCCTGA-3'; Mouse *Mmp12*: Forword: 5'-CTGCCCCATGAATGACAGTG-3', Reverse: 5`-AGTTGCTTCTAAAC-3')

ELISA

The concentration of CXCL1 (MKC008B, R&D), CXCL2 (MM200, R&D), IL6 (M60000B, R&D), IFNG (MZF00, R&D), and IL17A (M1700, R&D) in BALF supernatants or Lung homogenates, mouse cotinine (EA100902, OriGene) in serum, human anti-elastin (E01E0050, Bluegene) in plasma, and IL17A (BMS2017HS, Invitrogen) in induced sputum were determined with ELISA kits following the manufacturer's protocol.

Lung histology and determination of collagen deposition

The left lobes of lungs were fixed in 4% paraformaldehyde at 4℃ for 24 h. After paraffin embedding, the tissue sections were prepared (3 μm). Lung sections were stained with hematoxylin/eosin (H&E), PAS or Masson trichrome. The H&E staining sections were semi-quantitated (score: 0–4) with Olympus microscope (10 × 20 magnification) for the inflammatory situation. PAS stained goblet cells in airway epithelium were scored as described previously (3). Collagen area on the basal membrane of airway was analyzed by Leica-Qwin image-processing system (Leica Imaging Systems, Bensheim, Germany). The result was expressed as collagen staining area of per micrometer length of basement membrane of bronchioles. At least 10 bronchioles with 150 to 250 μm of internal diameter were counted on each slide. All slides were examined in a random blinded fashion by 2 independent investigators.

Immunohistochemistry and Immunofluorescence

Sections of lung tissues were immunostained with anti-MUC5AC, according to the manufacturer's instructions. Images were scanned with an Olympus BX53 inverted microscope (Olympus, Melville, NY), and image quantitative analysis was performed as

previously described [1]. MUC5AC positive bronchial epithelial cells were presented as a percentage of total epithelial cells.

Collection and processing of induced sputum

Sputum was induced as previously described [2]. A sample was considered adequate when the patient was able to expectorate at least 2 ml of sputum and the slides contained <10% squamous cells on differential cell counting. All sputum samples were kept at -80℃ until analysis.

Genotyping of HLA-A alleles

EDTA-anticoagulated peripheral blood from COPD patients or healthy controls were collected, and genomic DNA was extracted using a universal genomic DNA kit (CWbiotech, China) following the manufacturer's procedure. High resolution genotyping of HLA-A alleles was performed by Immunogenetics Laboratory, Blood center for Zhejiang Province using commercial polymerase chain reaction (PCR) plus sequence-based typing (SBT) kit (One Lambda, Inc.).

PBMC isolation

Heparin-anticoagulated peripheral blood from COPD patients or healthy controls were collected and centrifuged at 400 × g for 5 min and the top layer containing plasma was removed. The remaining blood was diluted with an equal volume of normal saline, 5 ml of diluted blood was layered over 5 ml of the Ficoll-Paque PLUS (GE Healthcare). Gradients were centrifuged at 400 × g for 30 min at room temperature in a swinging-bucket rotor without the brake applied. The PBMC interface was carefully removed by pipetting and washed with normal saline by centrifugation at 400 × g for 5 min. PBMC were prepared for further use.

GVAPGVGVAPGV/HLA-A*02:01 tetramer prediction, synthesis and staining

Epitope prediction was performed on 2018/4/20 with the IEDB Analysis Resource web interface [3, 4]. Briefly, the repeating peptide VGVAPG was input as specific sequence, all

possible sub-peptides (with 8-14 residues) hosted within the full-length were predicted to bind with all human HLA-A, -B, -C alleles in IEDB recommended 2.19 database. The predicted output is given in units of IC50 (nmol/l). Peptides with IC50 values <50 nmol/l are considered with high affinity. GVAPGVGVAPGV and HLA-A*02:01 were paired as they were among those with high or intermediate affinity in prediction, and HLA-A*02:01 is a common allele in human.

PE-conjugated GVAPGVGVAPGV/HLA-A*02:01 tetramer was synthesized according to the protocol published previously [5].

PBMC pellets were suspended and incubated in human T cell culture medium containing 5% autoplasma for 7 days in the presence of IL2 (R&D systems). Cells were then harvested and stained for GVAPGVGVAPGV/HLA-A*02:01 tetramer, anti-CD3, and anti-CD8 antibodies (eBioscience) for analysis of tetramer positive cells by flow cytometry.

Flow cytometry

Mouse lung white blood cells or human peripheral blood mononuclear cells were stained with indicated antibodies and were analysed by BD Fortessa LSR. The samples were analysed using the Flowjo software (Treestar LLC. Ashland, Oregon, USA). Anti-Mouse CD45 perCP-Cyanine 5.5, Anti-Mouse CD3e APC-Cyanine7, Anti-Mouse CD8a PE-Cyanine 7, Anti-Mouse CD4 PE-Cyanine7, Anti-Mouse IFNG FITC, Anti-Mouse IL17A APC, Anti-human CD45 APC, Anti-human CD8a eFluor®450, Anti-human CD3 PE-Cyanine 7, Anti-human IFNG Alexa Fluor®488, and Anti-human IL-17A PE were all purchased from eBioscience, San Diego, CA, USA.

Measurement of lung function

Mice were sedated with 0.1 g/kg intraperitoneal and 1% pentobarbital sodium, and the dose could be adjusted as necessary. The mice were intubated with a 2-in-long, 14-gauge angiocatheter which then connected to a rodent-specific forced maneuver system (Pulmonary Function Testing, Buxco Research Systems, USA). A series of preprogrammed forced ventilation maneuvers were used to measure FVC (forced vital capacity) and FEV_{20} (forced expiratory volume in 20 seconds) within 10 minutes. Each measurement was performed a

minimum number of three times to ensure reasonable repeatability.

Morphological analysis of lung sections

Serial longitudinal sections (3-µm thick) stained with hematoxylin/eosin (H&E) were used for morphological analysis. Ten randomly selected (100x) fields per slide were photographed using Olympus BX53 inverted microscope (Olympus, Melville, NY). The images were analyzed using the modified Image J software (open source), as described previously[6]. From each field, 10-12 areas of interest, free of airways and blood vessels, were picked for measurement of the number of intersections of virtual lines of known length, with alveolar septa. An increase in the average distance between intercepts (mean linear intercept) indicates enlarged airspaces.

Statistical analysis

One-way analysis of variance (ANOVA) was used to analyze the statistical differences among the groups, with P values indicated in the related graphs. Differences between 2 groups were identified using the Student's t-test. All data are expressed as mean ± s.e.m.. The analyses and graphs were performed using GraphPad Prism 7.0 software (GraphPad Software Inc., San Diego, CA, USA). A value of P less than 0.05 was considered statistically significant.

Reference

1. Chen ZH, Wu YF, Wang PL, Wu YP, Li ZY, Zhao Y, Zhou JS, Zhu C, Cao C, Mao YY, Xu F, Wang BB, Cormier SA, Ying SM, Li W, Shen HH. Autophagy is essential for ultrafine particle-induced inflammation and mucus hyperproduction in airway epithelium. *Autophagy* 2016: 12(2): 297-311.

2. Kips JC, Fahy JV, Hargreave FE, Ind PW, in't Veen JC. Methods for sputum induction and analysis of induced sputum: a method for assessing airway inflammation in asthma. *The European respiratory journal Supplement* 1998: 26: 9s-12s.

3. Lundegaard C, Lamberth K, Harndahl M, Buus S, Lund O, Nielsen M. NetMHC-3.0: accurate web accessible predictions of human, mouse and monkey MHC class I affinities for peptides of length 8-11. *Nucleic acids research* 2008: 36(Web Server issue): W509-512.

4. Nielsen M, Lundegaard C, Worning P, Lauemoller SL, Lamberth K, Buus S, Brunak S, Lund O. Reliable prediction of T-cell epitopes using neural networks with novel sequence representations. *Protein science : a publication of the Protein Society* 2003: 12(5): 1007-1017.

5. Rodenko B, Toebes M, Hadrup SR, van Esch WJ, Molenaar AM, Schumacher TN, Ovaa H. Generation of peptide-MHC class I complexes through UV-mediated ligand exchange. *Nat Protoc* 2006: 1(3): 1120-1132.

6. Chen ZH, Lam HC, Jin Y, Kim HP, Cao J, Lee SJ, Ifedigbo E, Parameswaran H, Ryter SW, Choi AM. Autophagy protein microtubule-associated protein 1 light chain-3B (LC3B) activates extrinsic apoptosis during cigarette smoke-induced emphysema. *Proc Natl Acad Sci U S A* 2010: 107(44): 18880-18885.

Supplementary Figure 1. Dose-dependent effects of elastin challenge in inducing airway inflammation. Mice were sensitized with air or CS, and then challenged with various doses of elastin (25, 50, or 100 μg) intratracheally (i.t.) for 3 times. Mice were sacrificed 48 h after last elastin instillation, and the inflammatory cell counts (**a**) and cytokines (**b**) in BALF were detected. Mac: macrophages; Neu: neutrophils; Lym: lymphocytes; Eos: eosinophils. Throughout, data are representative of 5 mice and were replicated in at least 3 independent experiments. Data are mean ± s.e.m. *P < 0.05, **P < 0.01, ***P < 0.001 by one-way ANOVA.

Supplementary Figure 2. FACS Gating strategy for identification of T cell responses in mouse lung single cell suspension. Mouse lung single-cell-suspensions were harvested and stained with fixable viability stain to exclude dead cells, mouse anti-CD45, anti-CD3, anti-CD8 were labeled to identify T cells and mouse anti-IL17A, anti-IFNG antibodies were label after fixation and permeabilization to detect specific T cell responses. Plot (**a**) Total cells. Plot (**b**) Single cells. Plot (**c**) Live $CD45^+$ white blood cells. Plot (**d**) $CD3^+CD8^+$ represents Tc subsets while $CD3^+CD8^-$ represents Th subsets. Plot (**e.f**) $IL17A^+$ represents Tc17/Th17 subsets while $IFNG^+$ represents Tc1/Th1 subsets.

Supplementary Figure 3. Sensitization and short-term challenge with mouse elastin induce Th1 immune responses and a bronchitis-like airway inflammation in mice. (**a**) Experimental outline. Mice were sensitized with elastin (Eln, 100 μg) and CFA or normal saline (NS) intraperitoneally (i.p.) at day 1 and 14, challenged with elastin (100 μg) intratracheally (i.t.) for 3 times at day 29, 30, and 31, and sacrificed 48 h after the last elastin challenge. (**b**) Inflammatory cell counts in the BALF. (**c**) Representative images of H&E staining and the semi-quantified scoring of mouse lung sections. (**d**) Concentrations of CXCL1, CXCL2 and IL6 in BALF. (**e**) Levels of Th1, Tc1, Th17, and Tc17 in mouse lungs. (**f**) Levels of IFNG and IL17A in mouse lung homogenates. (**g**) Expression of *Muc5ac* mRNA transcripts in mouse lungs. (**h,i**) Representative images and the semi-quantified scorings of PAS (**h**) or MUC5AC (**i**) staining in mouse lung sections. Mac: macrophages; Neu: neutrophils; Lym: lymphocytes; Eos: eosinophils. Throughout, data are representative of 5-6 mice and were replicated in at least 3 independent experiments. Data are mean ± s.e.m. *P < 0.05, **P < 0.01, ***P < 0.001 by one-way analysis of variance

(ANOVA).

Supplementary Figure 4. *Rag1*$^{-/-}$ mice exhibit little mature CD3^{+} cells in lung. Representative flow cytometry images showing the depletion of CD3^{+} cells in WT and *Rag1*$^{-/-}$ mice lung tissue single-cell suspension.

Supplementary Figure 5. Repeated CS exposure/rest cycle enhance the T cell response to elastin. Mice were subjected to CS exposure/rest for two cycles, lung red-blood-cell-free single-cell-suspensions were cultured in the presence or absence of elastin for 72 hrs, (**a. b**) cell culture supernatants were collected for ELISA analysis. Data are representative of 5 mice. Data are mean ± s.e.m. *P < 0.05, **P < 0.01 by one-way ANOVA.

Supplementary Figure 6. Exposure to CS for 6 months induces emphysema-like phenotype in mice. Exposure to CS for 6 months induces emphysema-like phenotype in mice. **(a)** Inflammatory cell counts in the BALF. **(b)** Representative images of Masson's trichrome staining of mouse lung sections and the semi-quantified scoring. **(c)** Representative images of PAS staining of mouse lung sections and the semi-quantified scoring. **(d)** Representative images of airspace and measurement of the MLI of mouse lungs (n=16). Mac: macrophages; Neu: neutrophils; Lym: lymphocytes; Eos: eosinophils. Throughout, data are representative of 7 mice unless otherwise indicated, and were replicated in at least 3 independent experiments. Data are mean ± s.e.m. ***P < 0.001 by student's *t*-test.

Supplementary Figure 1

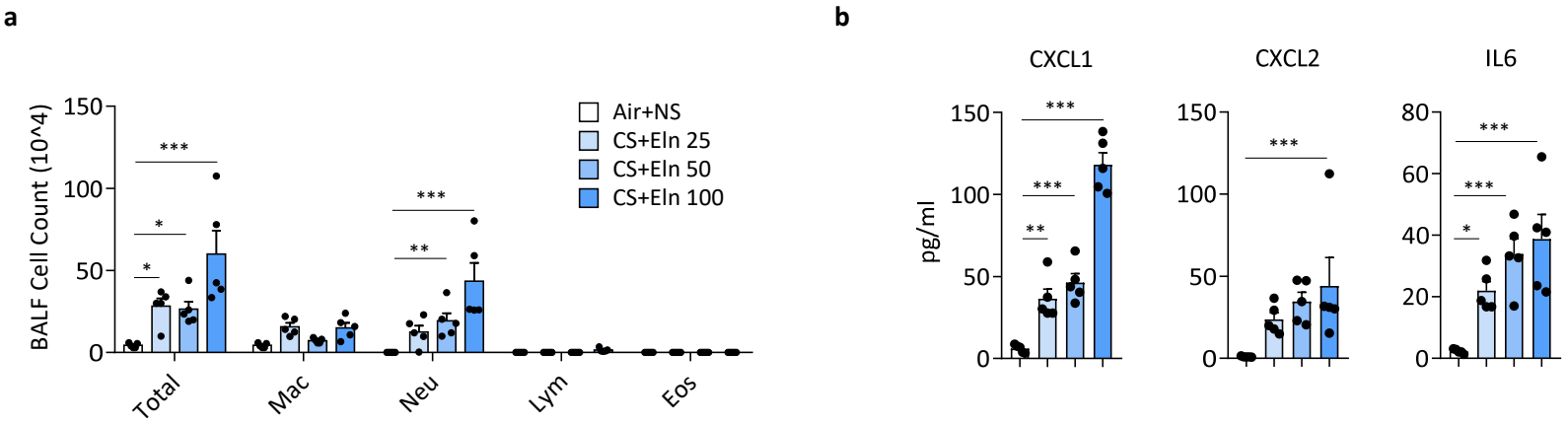

Supplementary Figure 2

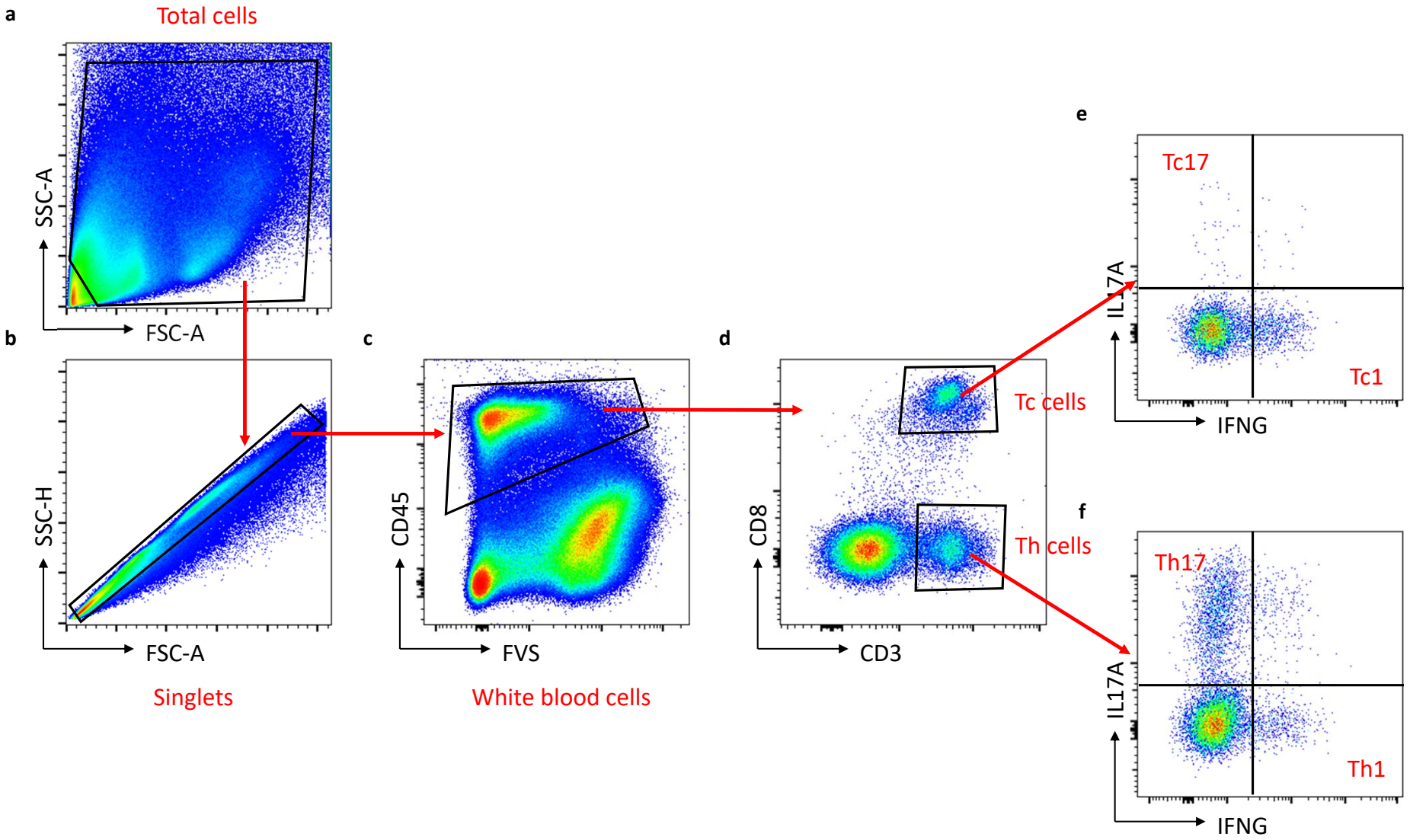

Supplementary Figure 3

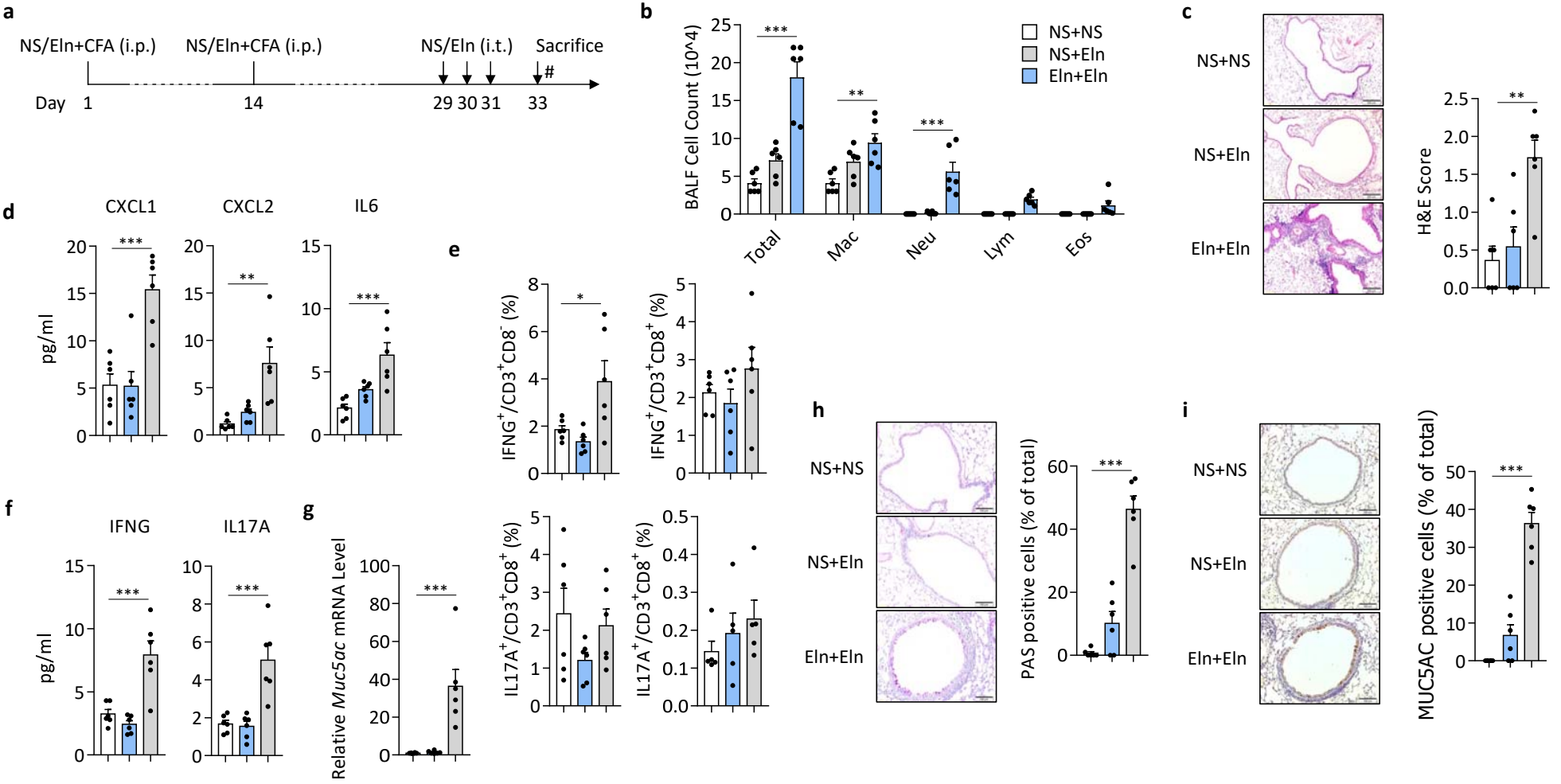

Supplementary Figure 4

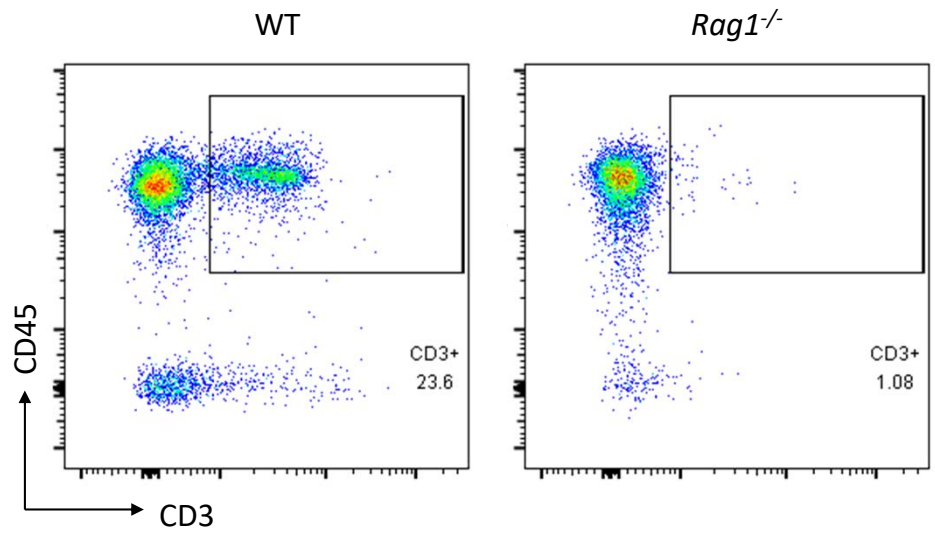

Supplementary Figure 5

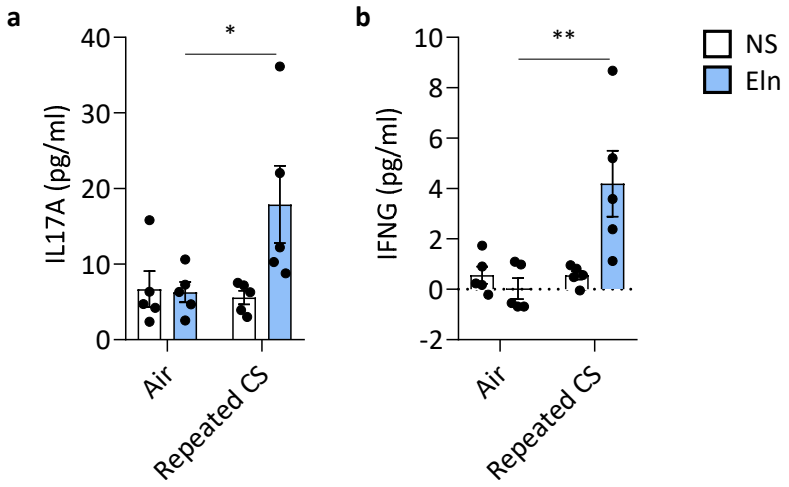

Supplementary Figure 6